CODEN:LUTEDX/(TEAT-5040)/1-51/(2000)

Shielding Methods for Radio Frequencies

Anton Brink

Department of Electroscience
Electromagnetic Theory
Lund Institute of Technology
Sweden

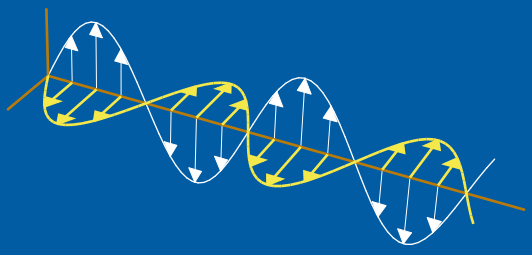

Handledare: Daniel Sjöberg
Per-Anders Svensson, Ericsson Mobile Communications AB

Editor: Gerhard Kristensson

Abstract

The result of this thesis is a functional shield test measurement system and a written part with gathered shielding theory. The system can be used for evaluation of shielding materials before they are introduced in the development of mobile phones.

There are demands from ITU (International Telecommunication Union) specifying limits for spurious emissions from devices using telecommunications standards such as GSM (Global System for Mobile communications). The need for shielding in mobile phones has driven Ericsson Mobile Communications AB to initiate this thesis regarding shielding. In order to make the mobile phone development smooth; the development engineers must have solid ground to base their statements upon when choosing shielding materials. The solid ground consists of better understanding of shielding theory and a measurement system for testing the intrinsic shield material properties and the performance of the joints between different shielding materials. A late discovery of deficient shielding in a mobile phone project can be very costly due to possible delayed market launch.

The thesis starts with a shielding theory part. In this part an extensive shielding theory has been collected from available public sources. The shielding theory part starts with an introduction to shielding foundations and the effect of a gasket in the shielding enclosure. Further is a study of apertures and other radiation sources. This part ends with a section about practical shielding.

The second part of this thesis describes the design of the shield test measurement system. The process leading to the functional measurement system is described. The parts of the system are also described here.

The test system can perform relative shielding effectiveness measurements. The measurement results can be used for an evaluation regarding which shielding material to use in a mobile phone project. The results from the measurement system are stable and repeatable.

The functional measurement system is the result of hard work. The progress of the design work for the shield test measurement did not always go smooth. A lot of problems were discovered in the system verification process, and the most important are reported in this thesis. However, at the end, a functional system appeared.

Preface

The purpose of this Master's thesis is to investigate existing shielding theory and to design a usable test system for measurements of shielding effectiveness.

The work has been carried out at GUB/DR Ericsson Mobile Communications AB, Lund, Sweden, during the period, the 18th of September 2000 to the 2nd of March 2001.

Lund, March, 2001

Anton Brink

1 Introduction

This thesis was initiated by Ericsson Mobile Communications AB ("Ericsson"). Ericsson had a need of better understanding of shielding phenomena. It would also be valuable for Ericsson to have a platform for measuring shielding effectiveness in order to know more about different types of shielding materials offered by manufacturers, before the materials will be used in the design of new mobile phones. Those factors combined led to this thesis in Electrical Engineering called Shielding Methods for Radio Frequencies.

1.1 Purpose

The purpose of this thesis was to do an investigation of existing shielding theory, and to design a shielding effectiveness test platform. In order to find shielding theory, an extensive library search was performed. The shielding effectiveness test platform is designed with support from the shielding theory. To obtain relevant measurements of shielding effectiveness, a realistic test environment must be created in means of contact resistance, edge effects, diffraction, reflections, cavity resonance, multi-moding and interference.

1.2 Disposition

The thesis consists of two parts: one theoretical part about shielding theory, and one part about design and verification of a test platform for measurements of shielding effectiveness.

The theoretical part consists of an explanation of shielding theory and the generation of electric and magnetic fields. It also contains some useful formulas for theoretical estimation of shielding effectiveness. The theoretical part guides the practical selection and evaluation of shielding materials and the geometry of the shielding.

The design and verification part consists of a discussion of the thoughts initiating the design of the test platform and the proceedings leading to the completed test platform. The test system is used for testing two shielding materials. The verification part includes the evaluation of the results from the measurements.

2 Shielding Theory

2.1 Shielding Foundations

This section starts with an explanation of interference phenomena and different approaches to describe the effect of the shielding. The rest of this section explains some basic conceptions regarding shielding and waves.

The first passage about electromagnetic interference explains why there is a need for shielding. The following passage gives insight in the shielding effectiveness concept. In this first part of the thesis there are also descriptions of what is happening physically in the shield and different approaches for how to describe the shielding. The last passage describes the difference between far fields and near fields.

2.1.1 Electromagnetic Interference

Electromagnetic interference, EMI, is a problem in most electrical circuit constructions. The problem consists of radiated or conducted energy that adversely affects circuit performance [3]. Unwanted signal interference may cause malfunction in the function of the circuit. In order to design reliable circuit functions the signal interference must be avoided. EMI can be reduced in two ways; a circuit can not radiate too much energy and a circuit must tolerate some incident radiation.

The circuit designer must be aware of the environment his design will be used in. The designer must also be aware of the need of limiting the radiation from the circuit. One must make sure the construction is unaffected by the surrounding electromagnetic fields and the designer must also make sure the design does not contribute to the electromagnetic surroundings in a harmful way. The EMI can leave or enter an electronic circuit in two ways. It can pass through a radiated path or a conducted path. The radiated path is through gaps, slots, openings or other discontinuities that may be present in the housing structure. Conducted signals are coupled onto the power, signal and control lines leaving the housing where they are free to radiate in open space, causing interference [8].

Regulatory agencies in states all over the world consider EMI issues very important. The agencies make regulations that intend to limit the electromagnetic fields that are radiated from electronic devices. The intent of these regulations is to reduce or control the electromagnetic "pollution" that is created by these emissions for the ultimate purpose of controlling the interference they create with other electronic devices. Even if the limits from the regulations are reached it does not guarantee that there will be no interference, it is only less likely. It is illegal to sell a product not compliant to these demands from the regulatory agency [13].

Regarding EMI issues the highest frequency of radio frequency (RF) emissions is usually the most critical because it has the smallest wavelength. It is also important to take into account any harmonics that may be present. Small wavelength is critical since even very tiny slits can act as apertures in the shielding. This is explained later in this thesis.

2.1.2 Shielding Effectiveness

The need for shielding is because we do not want frequency sources to propagate their radiation to unwanted places. To prevent occurrence from this, an enclosure must be put around the radiating device. A schematic picture of this is presented in Figure 1. It is also possible to work

the other way round, encapsulating the device that is getting jammed instead of the jamming device. In practice it is necessary to do both. It is very important to shield all radiating sources because if not a very dirty environment of radio frequencies will occur.

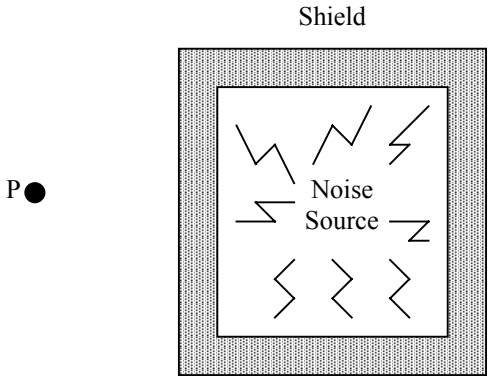

Figure 1. Shielding of noise source [12, p. 160]
The shield reduces the noise.

The shield makes an electromagnetic enclosure of the area of interest. Without the shield there would exist a vector electric field strength E_1 and a vector magnetic field strength B_1 at point P. The vector is fixed in its spatial orientation with its magnitude varying at the frequency *f*. With the shell at place the electric field strength at point P will have the new value E_2.

The electric and magnetic field at the point P are generally changed in direction and magnitude in the presence of the shell. An electric shielding effectiveness, S_E, and a magnetic shielding effectiveness, S_M, are defined as [6]:

$$S_E = 20 \cdot \log_{10} \frac{|\overline{E}_1|}{|\overline{E}_2|}$$

$$S_M = 20 \cdot \log_{10} \frac{|\overline{B}_1|}{|\overline{B}_2|}$$

2.1.3 Physical Screening Mechanisms

Two categories of physical mechanisms exist whereby a material shell can “screen” or “shield” a point P.

1. The bulk polarisation or magnetisation of the shell material, which can be loosely thought of as the “attraction” of either the electric E or the magnetic B field lines into the thickness of the shell, thereby weakening the field in its interior.
2. The establishment of oscillating or circulating currents in the material of a conductive shell, thereby producing electromotive or magnetomotive force fields, which oppose the original fields and tend to “expel” field lines from the volume of space occupied by the shell.

The second mechanism is the most important, except possible at very low frequencies where “magnetostatic” screening is achieved by shells of high permeability materials [8].

2.1.4 Near Fields, Far Fields and Plane Waves

Radiating electromagnetic waves consist of both an E-field (electric) and an H-field (magnetic) oscillating at an angle to each other. The ratio of E-field intensity to H-field intensity is called the wave impedance Z_W, see Appendix B. A device operating with a small current generates waves with high impedance. They are considered E-fields. Conversely, if a device contains a large current flow compared to its voltage, it generates low impedance H-field. Examples of devices generating E-fields are voltage sources, such as logic circuits and examples of H-fields generating devices are current sources, such as power amplifiers and motors [9].

Fields closer than $\lambda/2\pi$ from the radiating object are called near fields and more distant fields are far fields [3].

Figure 2 illustrates that wave impedance depends on the type of source and the observation distance from the source, r, referenced to the wavelength, λ, at the frequency of interest.

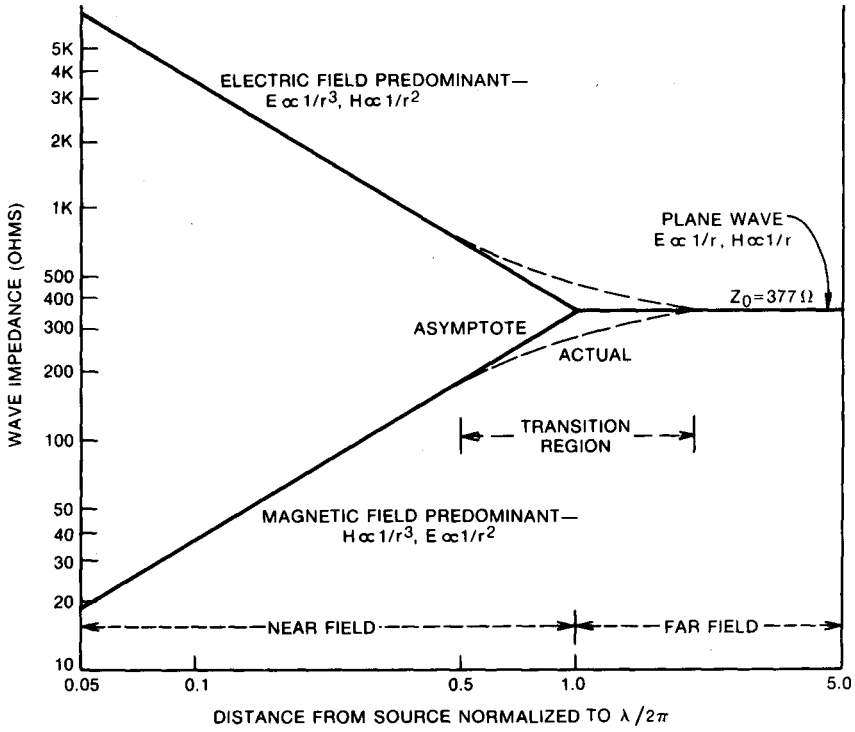

Figure 2. Wave impedance [12, p. 161]
The field characteristic is depending on its distance from the source and whether the field is electric or magnetic.

For air (σ=0, μ=μ_0, ε=ε_0), the characteristic impedance is Z_0=377Ω.

$$Z_{PlaneWave} = \sqrt{\frac{j\omega\mu}{\sigma + j\omega\varepsilon}} = \begin{bmatrix} \sigma = 0 \\ \mu = \mu_0 \\ \varepsilon = \varepsilon_0 \end{bmatrix} = \sqrt{\frac{\mu_0}{\varepsilon_0}} \approx 377\,\Omega$$

At the distance of $\lambda/2\pi$ from the radiating source, the ratio of E- to H-field strength approaches Z_0 regardless of their origin. When this occurs, the wave is said to be a plane wave, and the wave impedance is equal to 377 ohms, which is the intrinsic impedance of free space [3].

2.1.5 Wave Impedance Approach

The wave impedance Z_W of a propagating electromagnetic wave is defined as the phasor ratio of the electric field E to the magnetic field H, studied in Appendix B. This approach is useful because we can often establish an analogy between the propagation of voltage and current waves on transmission lines and the propagation of electric or magnetic fields through physical media.

The theory can be illustrated as an infinite flat plate of conductive material interposed between a source S and a point of measurement P. The distance from the source is assumed large in terms of wavelengths. An almost plane wave with electric field amplitude E_1 is propagating towards the right-hand plate surface. The region to the right of the plate can be seen as a lossless transmission line with a characteristic impedance Z_0=377Ω. Inside the plate material the propagating wave has the wave impedance given by the intrinsic impedance of the material. The plate is analogous with a transmission line with characteristic impedance.

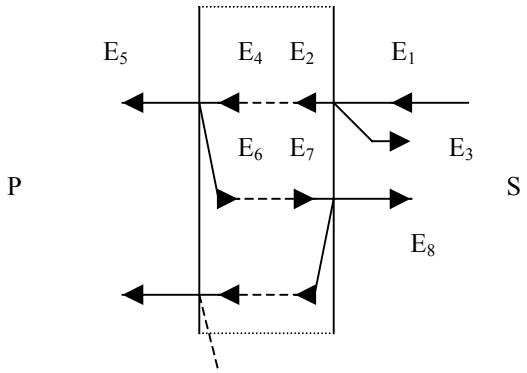

Figure 3. Transmission and reflections of plane wave in shielding material [6, p. 9]

The shielding material has a propagation constant $\gamma = \sqrt{j\omega\mu\sigma}$, a length *d* and characteristic impedance $Z = \sqrt{\mathrm{j}\omega\mu/\sigma}$. When a wave is propagated from the left side of the shield towards the shield some of the wave E_1 will be reflected at the shield shell (E_3) and some will be propagated (E_2). E_3 is given by $E_1 \cdot \frac{(Z_r - 1)}{(Z_r + 1)}$ and E_2 by $E_1 \cdot \frac{2Z_r}{(Z_r + 1)}$, where $Z_r = \frac{Z}{Z_W}$.

The following formula is derived in Appendix C from Figure 3.

$$E_P = E_1 \cdot e^{-\gamma d} \cdot \frac{4Z_r}{(1+Z_r)^2} \cdot \left[1 - \frac{(1-Z_r)^2}{(1+Z_r)^2} \cdot e^{-2\gamma d} \right]^{-1}$$

$\mathrm{d} = \mathrm{Shield\,width}$

$\delta = \mathrm{Skin\ depth\ (Appendix\ B)}$

The factor $e^{-\gamma d}$ relates to the attenuation of the wave from the point it reaches the shield until it leaves the shield again. The factor $\frac{4Z_r}{(1+Z_r)^2}$ is due to the impedance mismatch between the wave and the shielding material. The term $\left[1-\frac{(1-Z_r)^2}{(1+Z_r)^2}\cdot e^{-2\gamma d}\right]$ is derived from multiple reflections inside the shielding material.

If the analysis were conducted for the magnetic field the same expression would be derived with H instead of E.

It is practical to take the logarithm of the formula and then add the terms that are relevant in the particular case.

$$S = S_E = S_M = A_T + A_R + A_B$$

$$A_T = 20\cdot\log_{10}\left|e^{\gamma d}\right| \approx 8.686\cdot d/\delta$$

$$A_R = 20\cdot\log_{10}\left|\frac{(1+Z_r)^2}{4Z_r}\right| \approx 20\cdot\log_{10}\frac{1}{4|Z_r|} \text{ if } Z_r << 1$$

$$A_B = 20\cdot\log_{10}\left|1-\frac{(1-Z_r)^2}{(1+Z_r)^2}\cdot e^{-2\gamma d}\right|$$

The term A_T shows that the attenuation is very dependent of the skin depth (Appendix B). The skin depth is a material dependent coefficient. The term A_R is large if the impedance difference between the incident wave and the shield is large. This is the case of electric fields and they are hence subject to great reflection losses.

A_T is termed the "transmission" or "absorption" loss due to a single passage of the wave through the plate; A_R is the "reflection loss", due to initial reflection at both surfaces; and A_B is the term that accounts for all the subsequent re-reflections, and can be either positive or negative. The utility of this particular factorisation of S lies in the fact that if A_T exceeds 10-15 dB, A_B becomes negligible; this is likely to occur in practice at frequencies sufficiently high for the plane-wave assumption to be a reasonable approximation [6].

Shultz [15] studies the reflection loss dependence of the source impedance. If the impedance ratio Z_R is small as in the case of magnetic waves the reflection loss is small. Hence the opposite occurs in case of electric waves. Since the reflection factor is low for magnetic waves it is quite hard to implement good shielding for them.

2.2 Gaskets

This section describes the effect of a gasket in a shielding. Issues described include contact resistance, radiation and a theoretical way to study the phenomena.

2.2.1 Effect of Gasket and Contact Resistance

The current flow through the shield including a gasket is illustrated in Figure 4. There are two ways of occurrence for electromagnetic leakage.

First, the incident field E_i induces a current in the shield. The incident energy will leak directly through the material if the conductivity of the gasket material in Figure 4 is assumed to be lower than the conductivity of the material in the shield. The current will therefore decay less in the gasket and it results in more current flow on the far side of the shield. The increased flow causes a larger leakage field on the far side of the shield than if the gasket were absent.

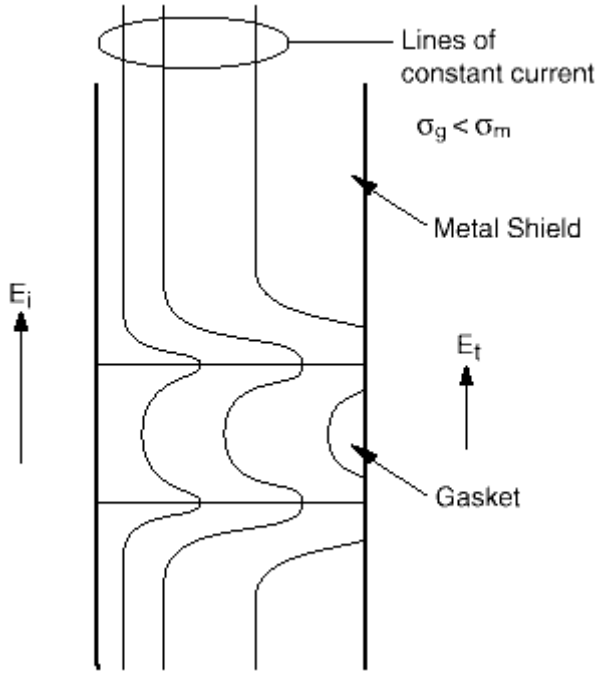

Figure 4. Lines of constant current flow through a gasketed seam [3, p. 3]
σ_{gasket} is lower than σ_{metal}

Second, the interface between the gasket and the shield can cause leakage. If an air gap exists at the interface, the current flow will be diverted to the points or areas in contact. The shielding performance will be lowered by this change in direction of the current distribution in the shield and in the gasket. A high resistance joint does not behave much differently than an open seam. [3].

The contact-resistance of gaskets determines ultimately the overall shielding efficiency. This statement is true, obviously, only if the other shielding component's efficiency is designed to be excessive. The selection of the most appropriate gasket type is a complex and critical task. Its consequences to the overall mechanical design should not be underestimated. [11, p. 566]

2.2.2 Gasket Radiation

A joint will radiate if there is a difference in potential between the housing surfaces. Figure 5 shows housing interrupted with a gasketed joint. The voltage across the joint is consistent with Ohms Law (Transfer Impedance) and is equal to the current J_S times the transfer impedance of the joint Z_T. The shielding effectiveness of the gasketed joint is equal to $20*\log (Z_W/Z_T)$.

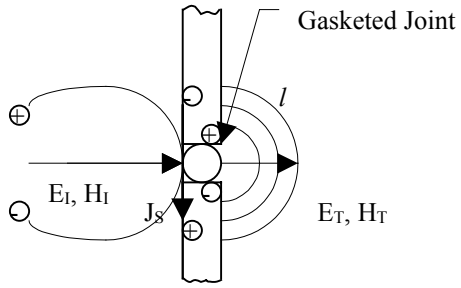

$$E_T \approx \frac{Z_T J_S}{l}$$

$$Z_T = \text{Transfer Impedance of Joint } [\Omega/\text{m}]$$

$$J_S = \text{Surface Current Density } [\text{A/m}]$$

$$H_T = \frac{2\pi R E_T}{Z_0 \lambda}, R < \lambda/2\pi$$

Figure 5. Gasket between shields [10, p. 276]
Radiation from a gasketed joint.

Figure 6 illustrates the EM field striking a solid conducting shielding barrier. The value of the surface current density J_{SI} on the incident side varies depending upon the impedance of the wave, the impedance of the barrier and the distance from the radiating unit to the barrier. The current density J_{ST} on the transmitted side is equal to the current on the incident side as attenuated by skin depth (Appendix B) [10].

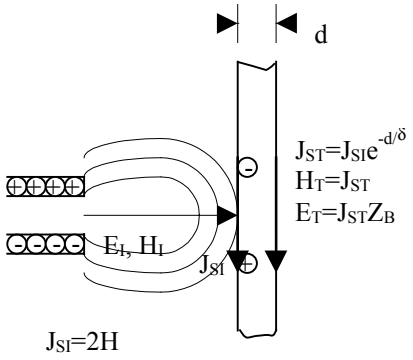

$$J_{SI} = \text{Current surface density on incident side of barrier } [\text{A/m}]$$

$$J_{ST} = \text{Current surface density on transmitted side of barrier}$$

$$Z_B = 1 + j/\sigma\delta(1 - e^{-d/\delta})$$

$$\sigma = \text{Volume conductivity of barrier } [\Omega/\text{m}]$$

$$\delta = \text{Skin depth } [\text{m}] \text{ (see Appendix B)}$$

$$d = \text{Thickness of barrier } [\text{m}]$$

Figure 6. Conducting shield barrier [10, p. 275]
Almost no radiation from a solid shield.

2.2.3 Transfer Impedance Approach

A way to study the impact of a joint is to study its transfer impedance. The transfer impedance is the impedance of the joint in the shielding. Figure 7 illustrates the fact that if a current flows through a non-zero impedance material, a voltage will be developed across the surface impedance and contact resistance. The shielding effectiveness (SE) is inversely proportional to the transfer impedance of the shielding.

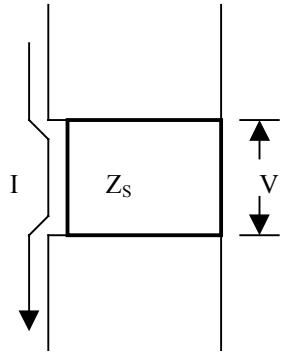

Figure 7. Transfer impedance of gasket [5, p. 30-9]

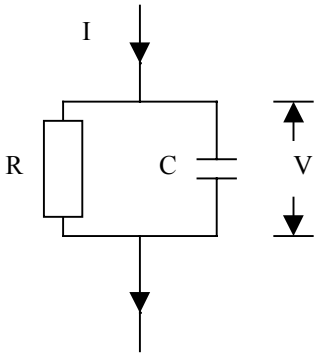

Figure 8. Lumped-element model of gasket [9, p. 85]

According to Jerse [9] the transfer impedance of a seam can be seen as a lumped-element model demonstrated in Figure 8. The seam is comprised of the parallel combination of a resistor and a capacitor. The resistor embodies the contact resistance between the two shield parts; the capacitor represents the electrical field coupling that occurs between the two closely spaced pieces of metal. The model demonstrates that a shield design with large contact resistance between its parts can be less effective at low frequencies than at higher ones.

The impact of transfer impedance is quite significant and often determines the effectiveness of the shield. In order to achieve good shielding the quality of electrical contact at the seams found between the shield parts must be high [9].

The transfer impedance concept emphasises the importance of providing a low impedance path for the surface current flow between shield parts. A significant degrade in shielding effectiveness occurs if a non-conductive substance is inserted in the seam such as corrosion [9].

If we model a gasket as seen in Figure 9, a transmission coefficient can be derived to be:

$$\tau = \frac{2Y_0}{Y + 2Y_0}.$$

The shielding effectiveness is expressed as: $SE = 20 \cdot \log_{10}\left(\tau^{-1}\right)$. If we then assume the admittance of the gasket to be equal to the inverted DC (0-frequency) resistance across the gap the expression will develop to (50-ohm line for an easy comparison to normal RF impedance):

$$\tau = \frac{0.04}{\frac{1}{R} + 0.04}$$

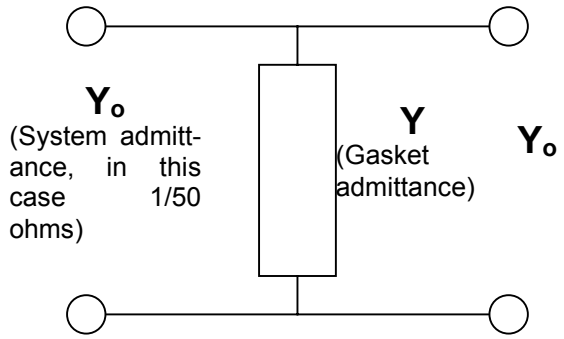

Figure 9. Lumped equivalent circuit of gasket junction. [4, p. 3] The connectors are equivalent to the shield materials lower and upper side with the gasket between.

The effect of the resistance R in the joint is illustrated in Figure 10. The illustration is only valid for low frequencies but since the principle is still valid for high frequencies the illustration is still useable. Material properties change by the frequency. The illustration is completely theoretical and can be computed by the following lines in Matlab [4]. (E.g. 50 Ohms)

```
R=[.01:.01:1];
Tau=(2/50)./((1./R)+(2/50));
LogTau=20*log10(1./Tau);
plot(R,LogTau);
```

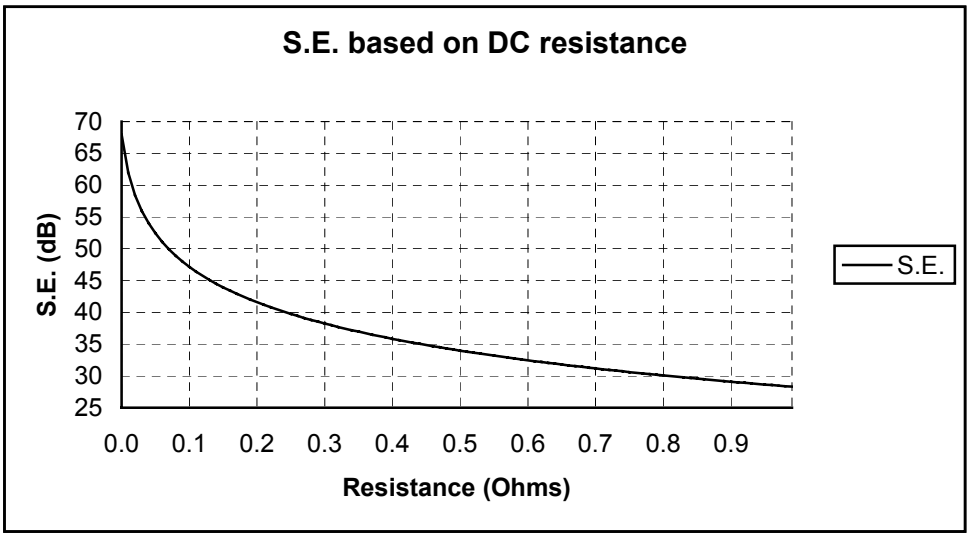

Figure 10. Predicted low-frequency shielding effectiveness based on DC resistance. [4, p. 3]

2.3 Apertures

2.3.1 General

Apertures are present in all practical shielding enclosures. The enclosures can not be solid because of the need for access covers, holes for conductors, ventilation and mechanical joints. All of these may considerably reduce the effectiveness of the shield. This means that the intrinsic shielding effectiveness is of less concern than the leakage through holes and seams. Leakage is often mainly depends on three items according to Ott [12]:

- The maximum linear dimension (not area) of the opening
- The wave impedance
- The frequency of the source

We study this using circuit theory approach to shielding. Noise fields induce currents in the shield; these currents then generate additional fields. The new induced fields cancel the original fields in some regions. There must be free paths in the material if this cancellation should be possible to occur. The further the current is forced to detour, the greater will the decrease in shielding effectiveness be.

To achieve a better understanding of the effectiveness of a shield it is useful to visualise the surface current flow around apertures and seams. A magnetic field, H, striking a metallic surface induces a surface current. In the ideal case the induced current would produce a corresponding field that is exactly equal but opposite to the impinging field on the other side of the surface. The ideal case would make the resulting flow on the surface of the shield zero and perfect shielding would be achieved. This theoretical condition corresponds to total reflection of the incoming wave [9].

Discontinuities in the shield surface that disrupt the current flow degrade the effectiveness of the shield. If a current is bending across a slot as shown in Figure 11, a voltage will be produced across the slot. The voltage will in turn couple a field to the other side of the shield. The reduction in shielding effectiveness is greater the more the discontinuity alters the intended path of the current flow. A series of holes as in Figure 12 would make less degradation of the shield than the slot in Figure 11, even though the holes encompass more surface area [9].

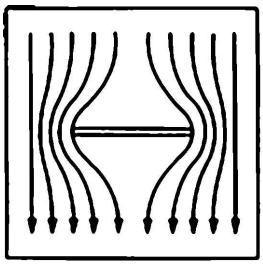

Figure 11. Current flow around one Slot [12, p. 188]

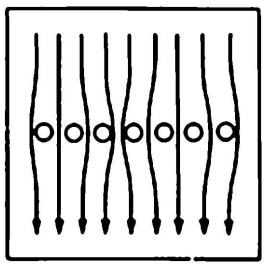

Figure 12. Current flow around Holes [12, p. 188]

For the worst-case polarisation of an incident wave, the shielding effectiveness of an aperture depends on its maximum linear dimensions (the length of the slot or the diameter of the hole) and not on its surface area [9].

2.3.2 Aperture Shielding Effectiveness Degradation

The main item determining the leakage from a slot is the maximum linear dimension (not area) of the opening [12]. Paying attention to how the slot length relates to the wavelength of the operating frequency of the circuit can be beneficial in shielding design [8].

Leakage also depends on the wave impedance and the frequency of the source. The highest frequency of RF emission is usually the most critical because it has the smallest wavelength. Then considering the highest frequency, it is important to take into account any harmonics that may be present [8].

After introduction of an aperture the following formula can be used to estimate the maximum possible shielding effectiveness:

$$S = 20 \cdot \log_{10}\left(\frac{\lambda}{2l}\right), l < \frac{\lambda}{2}$$

$$\lambda = wavelength$$

$$l = aperture\,length$$

This is applicable for slots with a dimension equal or less than half a wavelength. The equation shows that the shielding effectiveness is 0 dB when the slot is a half-wavelength long and increase 20 dB per decade as the length *l* is decreased. Reducing the slot by one-half increases the shielding by 6-dB [12].

2.3.3 Multiple Apertures

More than one aperture reduces the shielding effectiveness. The amount of reduction depends on [12]:

- The spacing between the apertures
- The frequency
- The number of apertures (n)

The SE degradation from multiple apertures of equal size can be estimated by the following formula:

$$S = -20 \cdot \log_{10}\left(\sqrt{n}\right)$$

or

$$S = -10 \cdot \log_{10}(n)$$

The shielding degradation is proportional to the square root of the number of apertures. The formula is only valid if the apertures are situated less or equal to a half wavelength from each other.

Apertures located on orthogonal surfaces radiate in different directions. Therefore it is advantageous to distribute apertures around the surfaces of the product to minimise the overall radiation.

2.3.4 Slits

A uniform wave is striking towards a sheet with a narrow slit as shown in Figure 13. E is perpendicular to the slit.

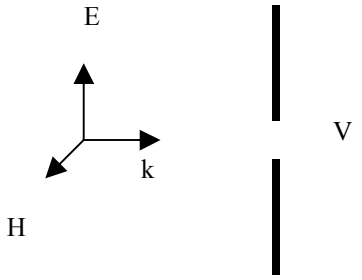

Figure 13. Slit [15, p. 49]
A wave is propagating towards a slit.

If there were no slit in the sheet the wave would be reflected and H would be doubled; the current density 2H will flow upwards in the plane. In presence of the slit complete reflection still occurs except in the region of the slit. The slit reduces the electric current to zero and a voltage is induced to reduce the current density to zero. This counter electromotive force produce charge concentrations on the edges of the slit [15].

2.3.5 Aperture Equation

We wish to calculate the radiation from a small area element Δs with dimensions Δx and Δy. The Fourier transforms will be simple to calculate because Δx and Δy are presumed to be very small.

$$\tilde{E}_y = \int_{-\Delta y/2}^{\Delta y/2} \int_{-\Delta x/2}^{\Delta x/2} E_0 e^{jk_x x'} e^{jk_y y'} dx' dy' \approx E_0 \Delta s$$

$$\tilde{H}_x = -(1/Z_0)\tilde{E}_y \approx -(1/Z_0)E_0 \Delta_s$$

Fourier transformation of the aperture distribution gives the pattern function.
After transformation from Cartesian co-ordinates to spherical co-ordinates and Fourier transformation the far field becomes:

$$E_\theta = \frac{j}{2\lambda}\frac{e^{-jkr}}{r} E_0 \Delta s(1+\cos\theta)\sin\phi$$

$$E_\phi = \frac{j}{2\lambda}\frac{e^{-jkr}}{r} E_0 \Delta s(1+\cos\theta)\cos\phi$$

These formulas are almost identical to those of a Huygen source, see [1].

2.3.6 Waveguide

If a hole in a shield has a diameter less than the shield thickness, a waveguide is formed (Figure 14). At frequencies below the cutoff frequency the waveguide works as an attenuator. The attenuation is a function of the length of the waveguide.

The lowest TE mode propagating through a circular waveguide is TE_{11} with cutoff frequency [14]:

$$f_{c_{11}} = \frac{1.841 \cdot c}{a \cdot 2\pi\sqrt{\mu_r \varepsilon_r}}$$

c = speed of light in vacuum

a = diameter of hole [m]

ε_r = relative permeability

The lowest TE mode propagating through a rectangular waveguide is TE_{10} with cutoff frequency [14]:

$$f_{c_{nm}} = \frac{1}{2\pi\sqrt{\mu\varepsilon}}\sqrt{\left(\frac{m\pi}{a}\right)^2 + \left(\frac{n\pi}{b}\right)^2} = \begin{bmatrix} m = 1 \\ n = 0 \end{bmatrix} = \frac{c}{a \cdot 2\sqrt{\mu_r \varepsilon_r}}$$

c = speed of light in vacuum

a = height

b = width

In a waveguide the attenuation below the cutoff frequency depends only on the ratio of length to diameter, see Figure 14. In thick shields it is possible to use the waveguide properties where penetration is necessary for some reason. If the shield is too thin it is possible to obtain a good length-to-diameter ratio by attaching a small metallic add-on shield e.g. a gasket of appropriate dimensions [8].

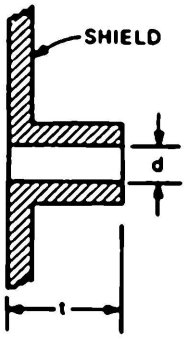

Figure 14. Waveguide model of a hole through the shield [8 , p. 192]

2.4 Other Radiation Sources

The first section describes the radiation from a closed circuit, the following section tells about the different strengths of radiation from common-mode and differential-mode currents.

2.4.1 Circuit Radiation

The area S an electric circuit surrounds creates an antenna that radiates, see Figure 15. The intensity of the radiation depends on the area S and the current distribution along the circuit. To understand the function of this antenna we can think of it as a receiving antenna. The incident wave causes a magnetic flux through S and induces voltage around the circuit [1].

If the length of the circuit is about 1 λ we have a resonant ring-antenna [1].

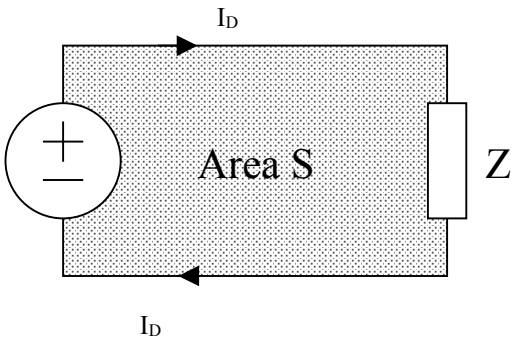

Figure 15. Inducted circuit area

2.4.2 Common-mode and Differential-mode Currents

Consider a two-conductor transmission line as illustrated in Figure 16.

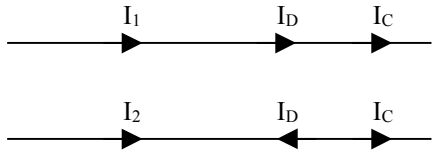

Figure 16. Current components in a transmission line
[13, p. 179]

The total phasor currents on the conductors directed to the right are designated I_1 and I_2. These can be decomposed into two current components.

$$\begin{aligned} I_1 &= I_C + I_D \\ I_2 &= I_C - I_D \end{aligned} \quad \Leftrightarrow \quad \begin{aligned} I_D &= \frac{I_1 - I_2}{2} \\ I_C &= \frac{I_1 + I_2}{2} \end{aligned}$$

This simple change of variables is significant with regard to the radiated emissions of the total currents. The current I_D is referred to as the differential-mode current and the current I_C as the common-mode current. The differential-mode current component, I_D, is equal in magnitude on both conductors but is directed in opposite directions at a cross section on the line. This is the functional or desired current that is assumed by the designers of the product. The common-mode current, I_C, is an undesired component of the currents and is not necessary for the functional performance of the product. These are sometimes referred to as antenna-mode currents. The common-mode currents are difficult to predict and their existence depends on nonideal aspect of the structure such as asymmetries.

Emissions of the common-mode current components are frequently larger than those of the differential-mode components. To see why this occurs, consider the radiated electric field of each

component shown in Figure 17 and Figure 18. Because the differential-mode currents are oppositely directed, their radiated electric field tend to subtract as shown in Figure 17. However, these fields do not exactly cancel, because the two conductors are not collocated. On the other hand, because the common-mode currents are in the same direction, their radiated fields tend to add as shown in Figure 18. Therefore a common-mode current component of considerably smaller magnitude than that of the differential-mode current can create the same level of emission.

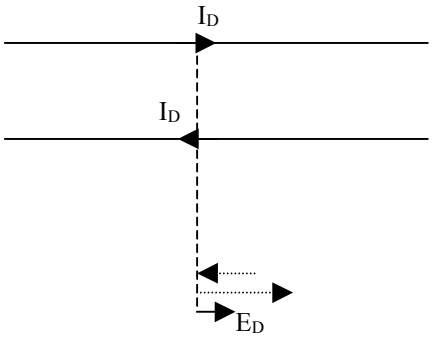

Figure 17. Radiation from differential currents is contrary to each other and tends to neutralise [13, p. 179]

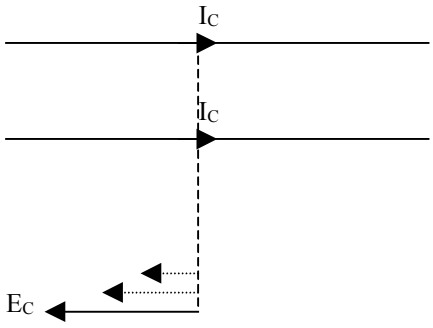

Figure 18. Radiation from common currents is equal in direction and tends to strengthen [13, p. 179]

There are two methods to reduce differential-mode current emissions:

- Reduce the current level and/or
- Reduce the loop area

Two methods to reduce common-mode current emissions are [13]:

- Reduce the levels of the common mode-current and/or
- Reduce the length of the conductors

2.4.3 Cavity Resonators

Cavity resonance is due to a shielding enclosure forming a reflecting cubicle of interior dimensions that are each some multiple of half-wavelengths. Under these conditions, interior fields are extremely non-uniform [15].

The resonance frequencies in a rectangular box are given by:

$$f_{mnl} = \frac{c}{2\pi\sqrt{\mu_r \varepsilon_r}} \sqrt{\left(\frac{m\pi}{a}\right)^2 + \left(\frac{n\pi}{b}\right)^2 + \left(\frac{l\pi}{d}\right)^2}$$

a = width

b = height

d = length

where the case $m = n = l = 0$ is forbidden.

Different modes having the same resonant frequency are called degenerate modes [2].

Microwave resonators are used in applications such as filters, oscillators, frequency meters and tuned amplifiers. Electric and magnetic energy are stored within the cavity, and power can dissipate in the metallic walls of the cavity as well as in the dielectric filling the cavity [14].

Inter-wall resonance can occur at the higher frequencies due to reflections between the conducting sheets of a double-shielded cavity when the frequency is such that the spacing between sheets is some odd multiple of quarter-wavelengths [15].

2.5 Practical Shielding

2.5.1 General

Shielding is always necessary in an enclosure because of the slots and gaps inherent in the structure. Good shielding at higher frequencies can usually be obtained by the use of thin-metal shielding as the case material. The assumption is that the shield makes a Faraday cage, meaning that the shield is continuos and fully surrounds the sensitive items without gaps or apertures.

There are several choices for joints between sheets that are permanently secured. Before joining the sheets, the surfaces must be clean to promote the complete filling of the joint with conductive metal.

Listed below are some performance criterions for selecting an EMI gasket to seal openings [8]:

- Shielding effectiveness over the specified frequency range
- Mounting methods and closure forces
- Galvanic compatibility with the housing structure and corrosion resistance to the outside environment
- Operating temperature range
- Cost

Medveczky makes the following observation in his article [11 p. 565]:

"The fact, however, that many EMC engineers, who are actively engaged in shielding enclosure designs, have more of a mechanical engineering than RF/microwave background, is often considered as the main reason for finding so many "shielding enclosures" with very poor shielding efficiency. This explanation, though valid in many cases does not address the whole problem. … Another cause of the prevailing confusion about EMC shielding is that there is neither time nor funding usually available for the EMC engineer, who is working in the industry, to make theoretical calculations and conduct scientifically valid measurements. … Typically, the EMC engineer is hard pressed to find some **quick fix** because the product is already scheduled for shipment."

By proper selection of type of material and the geometry of the shielding the gasketed seam will be "bridged". This means that the resulting performance of the shielding will approach that of a homogenous solid shield [16].

2.5.2 Materials

Existing design data show extremely high values for shielding against electric fields at low frequencies. Indeed they are so easy to shield against that the data are of little value as a measure

of performance. Actual shielding performance is normally less than the calculated values for not only the electric field but also for the magnetic field and plane waves. This result occurs because a practical shield is composed not only of a purely uniform material but of smaller sections of material joined together and with other features, such as penetrations, that violate the ideal situation of uniformity [15].

For higher-frequency electric fields, good shielding can usually be achieved by the use of thin metal shielding as the case material or lining, but the assumption is that the shield is continuous and fully surrounds the sensitive item without gaps or apertures (a Faraday cage). In reality, it is rarely possible to construct a shield without some type of joint or aperture. The shielding may have to be fabricated in pieces, and therefore it may have seams that must be joined. It is usually necessary to penetrate the shield for providing access to boards or to mount components [8].

Since the primary reflection occurs at the first interface for electric fields, even extremely thin shields of low impedance material can provide large reflection loss [5].

2.5.3 Measurements

The intrinsic shielding effectiveness of complex materials is difficult to predict theoretically. Therefore measured SE data are necessary [17].

The investigation in this thesis has not revealed a common measurement method useful for everyone. It seems like it is up to every user of shielding to find a measurement method that suits the specific needs of a specific customer. This is because of the differences in influence from near and far fields in different shielding applications. The specific geometry of the shielding cover may also matter for the differences in shielding effectiveness using the same materials. Tsaliovich [16 p. 417] also mention this fact:

"The proof of the shielding is in testing."

Suppose the SE of a plane sheet of material has been carefully measured via some theoretically sound test procedure. If this same material is used to form electronic equipment housing, then we may find that the SE of the container bears little relationship to that of the original plane sheet. The effects of finite size, geometry, corners, etc., can significantly alter the material's shielding ability [17].

Shielding effectiveness data on a single test sample obtained with one technique does not necessarily correlate with that obtained with another technique. Each technique will use it's own set of electromagnetic field impedance conditions and therefore will the obtained data not correlate between the different techniques. The supplier of candidate shielding materials must state the conditions under which the shielding effectiveness was measured; otherwise, the designer does not have sufficient data to determine whether or not a given material is appropriate for the intended application [5].

2.5.4 Attenuation

The attenuation provided by an RF shield results from three mechanisms [7]:

- Incident energy is reflected by the surface of the shield because of the impedance discontinuity of the air-metal boundary. This mechanism does not require a particular material thickness, but simply an impedance discontinuity. A special case exists when a gap in the shield has length, such as a honeycomb vent.

- Energy that cross the shield surface (i.e. not reflected) is attenuated (absorbed by turning into heat energy) in passing through the shield.
- The energy that reaches the opposite face of the shield encounters another air-metal boundary, and thus some of it is reflected back into the shield.

The part of the field that is transmitted across the boundary supports a current in the metal, as illustrated in Figure 19. The amount of current flow at any depth in the shield and the rate of decay are governed by the skin depth (Appendix B). The residual current appearing on the opposite face is the one responsible for generating the field that exists on the other side [3].

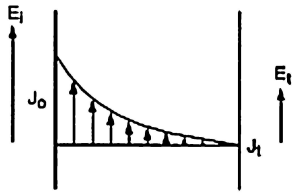

Figure 19. Skin depth attenuation
[3, p. 3]

3 The Design of the Measurement System

3.1 General Description

The purpose of the measurement system is to perform shielding effectiveness (SE) evaluations of new shielding materials for use in mobile phones. There used to be no proper method of how to select shielding materials when a mobile phone project demanded some kind of shielding.

Inside a mobile phone there are components working at radio frequencies. The leaking signals from one component can disturb other components or devices outside the mobile phone. The components are grouped in sections with special tasks. The sections are encapsulated in different cavities, which are intended to be shielded from each other. The components inside a cavity can also be disturbed from radiation sources outside the mobile phone.

The fundamental frequency is the problem internally in the mobile phone. The harmonics are a problem externally because they can be in the fundamental frequency range for other communication systems. Because of such possible problems, the ITU (International Telecommunication Union) specifies the maximum allowed levels for signals outside the fundamental frequency for a mobile phone.

Summary of the shielding cases regarding mobile phones:

- From cavity to cavity in the mobile phone
- From cavity to the surroundings outside the mobile phone
- From the surroundings to inside a cavity in the mobile phone

The shielding problems are usually discovered late in the development phase. If the problems are discovered too late, the mobile phone's market launch can be delayed, which is very costly. The measurement system treated in this thesis gives a possibility to test new shielding materials early in the design process.

The general function of a shield is to reduce the signal passing through the shield. Ideally the shield would not let any signals to pass. The shield function is illustrated in Figure 20. The transmitting antenna transmits a strong signal. The signal strikes a shielding material placed between the transmitting antenna and the receiving antenna. The signal passes through the shielding material but loses energy; the energy reduction is depending on the materials characteristic. A receiving antenna receives the signal. The transmitted power is compared to the received power, making it possible to tell how the material reduced the signal; referenced to a measurement without any shielding material between the antennas.

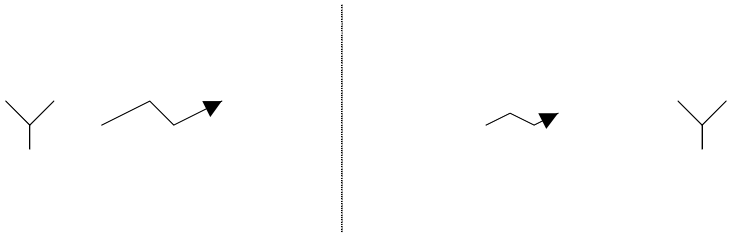

Figure 20. An antenna is transmitting a strong signal. The signal strikes a shielding material and loses energy. A receiving antenna receives the weakened signal.

The designed measurement system encapsulates the transmit antenna inside a shield test equipment. The shield test device functions as if the transmit antenna had a sphere made of shield test material around itself. At a distance from the shield test device a receiving antenna receives the weakened signal, see Figure 21.

Figure 21. The schematic shield test measurement system. 1. Shield Test Device, 2. Signal Generation Equipment, 3. Receiving Antenna, 4. Signal Detection Equipment

The shield test device and the receiving antenna are located in an anechoic chamber during the measurements. This arrangement shuts out the noise from other radiation sources, therefore ensuring a constant and well-defined environment. The design and verification process leading to a working shield test measurement system is described in this thesis. Two types of shield materials were used in the verification process; the shield materials are briefly described later.

3.1.1 Requirements

The specification for the shield test measurement system origins from discussions between the tutor, some experts and the author. The discussions regarded issues as; shielding theory, practical feasibility, experienced problems and the expected outcome of the design.

The overarching targets for the design were:

- The test environment must have similarities to the environment inside a mobile phone.
- The test system must be electrically tight; so the shielding material under test is the property deciding the radiation of the test system.
- Easy to apply new shielding materials.
- Flexible for new shielding cavity shapes.
- SE test by wave propagation through the shielding material and the joint to the board.
- Tests in the frequency range from 0.1 GHz up to 12.75 GHz[1].

3.2 The Measurement System

In this section there is first a brief description of the parts of the measurement system and then a thorough description of selected parts. The reasons for the introduction of certain parts are explained in following sections.

3.2.1 The Measurement System Parts

The Amplifiers

Two almost identical MITEC Low Noise Amplifiers (LNAs) had to be used in series to amplify the signal received from the RX (receiving) antenna before the signal was connected to the spectrum analyser. The first one was a MITEC AFS-3 and the second a MITEC AFS-4. The amplifiers combined gave an amplification of almost 50 dB.

[1] GSM specification frequency limits for measurements of spurious emissions.

The Anechoic Chamber
An existing shielded anechoic chamber was used for the measurements. The chamber is normally used for antenna pattern measurements. The use of an anechoic chamber made it possible to control the physical measurement environment in terms of radiation noise.

The Receiving Antenna
An EMCO conical log-spiral antenna model 3102L was used as RX antenna. The antenna performance is specified in the interval 1 GHz to 10 GHz; the antenna properties are not expected to change dramatically close to the specified limits.

The Shield Test Device
The shield test device is described in the following section.

The Signal Generators
Since the system is quite broad banded two signal generators had to be used. The HP 8657B was used in the frequency range 0.1-2060 MHz and the HP 8671B was used in the frequency range 2.0-18.0 GHz.

The Spectrum Analyzer
An HP 8596 spectrum analyzer was used as the detecting equipment for the test measurements.

3.2.2 The Shield Test Device

The illustration in Figure 22 shows the vital parts of the designed shield test device. An antenna strip in the bottom of the internal device volume transmits a signal. The internal device volume is electrically tight except for the cavity shape in top of it. A shield material cap can cover the cavity shape. At a distance from the shield test device a receiving antenna is located. With knowledge of the transmitted power and received power the materials shielding characteristic can be evaluated. By comparing the characteristic for several materials, this measurement system can be used for evaluations regarding which material to use in product development.

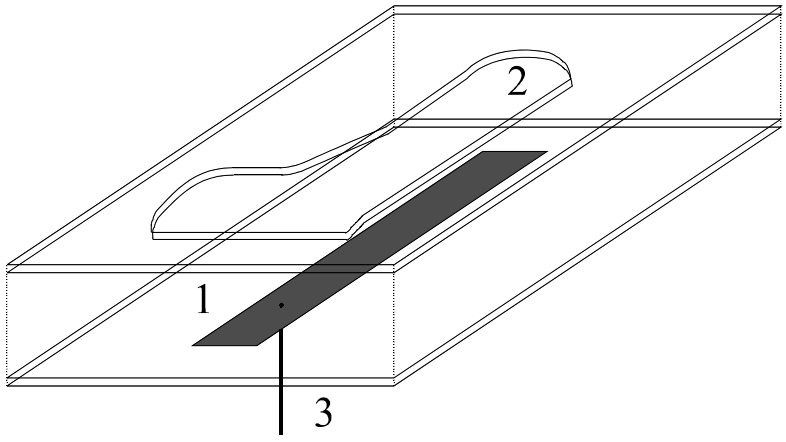

Figure 22. Schematic view of the shield test device. 1. Antenna Strip, 2. Cavity Shape, 3. Signal feed connection

The designed and manufactured shield test box can be studied in Figure 23 and Figure 24. The brass frame forms the walls of the shield test device. Brass is highly conductive and mechanically robust, making the material a good choice as base structure for the device. The physical dimension of the design was decided by assumptions from antenna experts, regarding sufficient

distance from the antenna strip to the brass frame and the shield material under test. The distance allows the antenna to function without changing its characteristic too much by the existence of metal in its close vicinity. The interior volume in the shield test device was decided to be 80*60*8 mm^3 (*l***w***h*). The outer brass frame dimensions are 10 mm bigger than the inner area dimensions. The height is 8 mm. The intervals between the screws are 14-15 mm.

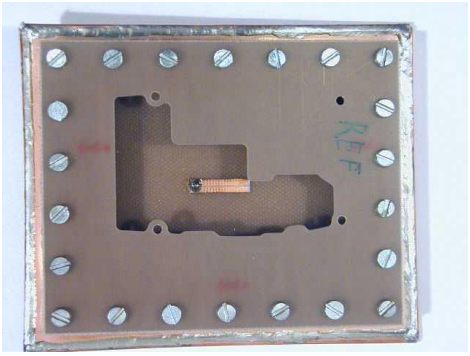

Figure 23. The shield test device.
Shield holding board mounted.

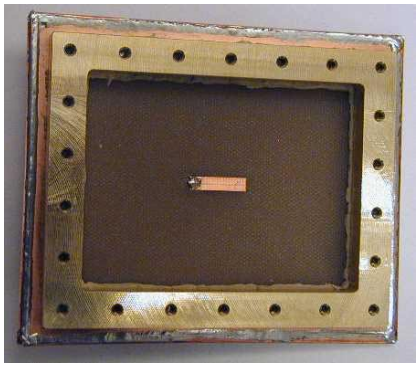

Figure 24. Transmit antenna.
Copper antenna strip on glass fibre substrate, mounted brass frame.

The antenna strip is located opposite to the cavity hole in the shield test device. The antenna development is closely documented in a following section. The form of the cavity shape was taken from the mechanical CAD (Computer Aided Design).

The top of the shield test device is the shield holding board, see Figure 25. The shield holding board is a glass fibre substrate with copper layer on one side. An opening was made in the board in the same form as an existing mobile phone cavity. The shielding material is applied to the copper side of the board in such way that the cavity shape is completely covered. The shield holding board was fastened to the brass frame with the copper side of the board in contact with the brass frame. This design ensures proper electrical contact between all parts. To improve the electrical contact, conductive grease was used in the joints between the board and the brass frame.

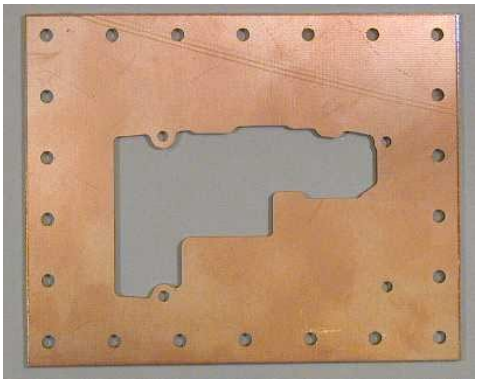

Figure 25. Shield holding board
The holding board is ordinary glass fibreboard with one copper layer.

Two shield materials were used in the tests of the shield measurement system:

- Steel cap: A shield cap manufactured of steel and a conductive silicone-rubber gasket, see Figure 26.
- Plastic cap: A shield cap manufactured of plastic material with metal particles, see Figure 27.

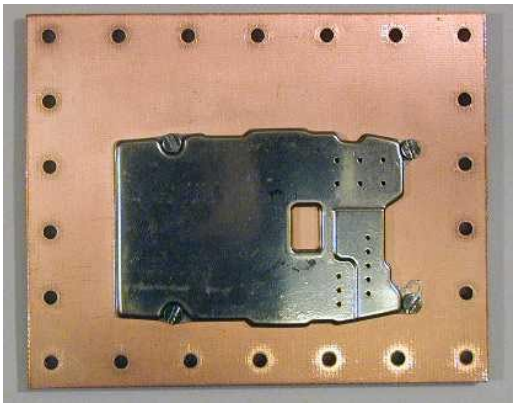

Figure 26. Steel cap.

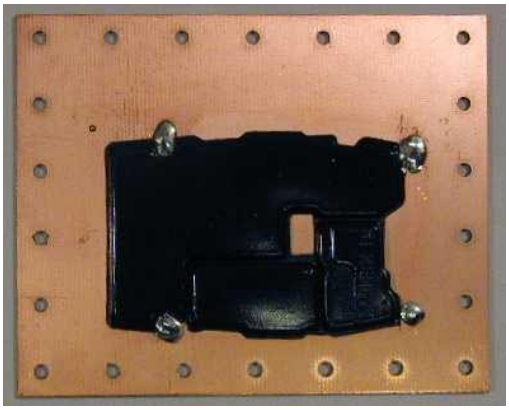

Figure 27. Plastic cap.

3.2.2.1 The Shield Test Device Parts and Assembly

The Antenna Board
The antenna board is thoroughly described in the following section.

The Brass Frame
The antenna board is mounted on a brass frame that holds the shield holding board.

The Shield Holding Board
The shield holding board is the board holding the shield material under test.

The Shield Cap
The shield cap is made of the material we would like to test in the test system.

The Assembly
The shield holding board and the antenna board are assembled to the brass frame with M3 screws. All screws are tightened to 0.5 Nm with moment screwdriver. The shield cap is applied to the shield holding board with screws or other methods depending on the shield material properties.

3.2.3 The Antenna Design

The specified frequency band from 0.1 GHz to 12.75 GHz is impossible to cover with one antenna designed on a thin glass-fibre substrate. Since the shielding effectiveness was not expected to change very much in narrow frequency intervals there was no need for measurements at a continuous frequency spectrum over the specified frequency band. The antenna frequencies were limited to 0.9 GHz, 2.4 GHz, 5.0 GHz, 9.0 GHz and 12.0 GHz. Those frequencies cover the fundamental frequencies of GSM and its harmonics.

The individual antenna was supposed to be matched to 50 Ohms at its working frequency. A matched antenna is characterised by low SWR (Standing Wave Ratio), ideally SWR=1, see Appendix B.

The antenna design resulted in a solution illustrated in Figure 28. The antenna strip is located on a glass-fibre substrate with a solid sheet of copper on the opposite side. The copper sheet acts as ground plane for the antenna; since the distance from the antenna strip to the ground plane is short the antenna is narrow banded. The antenna is signal fed from the bottom through a hole in the substrate.

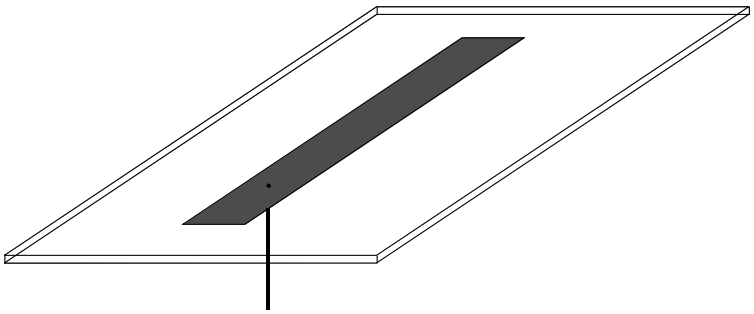

Figure 28. The antenna strip is placed on top of a glass-fibre substrate. The opposite side of the substrate is a solid copper sheet acting as ground plane for the antenna. The antenna is fed from the copper side of the substrate through a connector.

Two types of antennas were used in the design. PIFA (Planar Inverted F Antenna) and patch antennas. The different antenna types can be studied in Appendix D.

PIFAs were designed for the lower frequencies and patch antennas for the higher frequencies. The change of antenna model depending on working frequency was motivated by the practical feasibility of antenna manufacturing. The PIFAs are quarter-wave antennas with signal feed and ground connection arrangements that are hard to realise when the antenna length gets short at high frequencies. The patch antennas used at higher frequencies were chosen to be half-wave antennas, making them easier to physically realise in the manufacturing.

With knowledge of the approximate antenna lengths for the selected frequencies the antenna simulations could start.

3.2.3.1 The Antenna Simulations

The simulations were performed by use of the antenna simulation software IE3D from Zeland Inc. Before the simulations start the software needs to know about the material properties of the materials used for antenna manufacture and a rough sketch of the antenna. The information needed for the simulations are:

- Layout co-ordinates.
- Electrical properties of substrate layers, e.g. ε_r.
- Electrical properties of metal layers, e.g. conductivity.
- Application frequencies.

The initial layout co-ordinates did origin from the expected antenna lengths as known from shielding theory. The electrical properties of the glass-fibre substrate must be considered when the expected antenna lengths were calculated.

After every simulation the impedance match was studied in a viewed Smith chart. After a few rounds of simulations it was understood how a change of parameters affected the impedance match. The possible parameters to adjust were length, width and the distance from one of the narrow antenna ends to the signal feed point. After the initial trial-and-error phase the simulations went smooth. The purpose of the simulations was to find the antenna dimensions giving a 50 Ohms impedance at the supposed frequency; it is the centre point of the Smith chart, as seen in Figure 29.

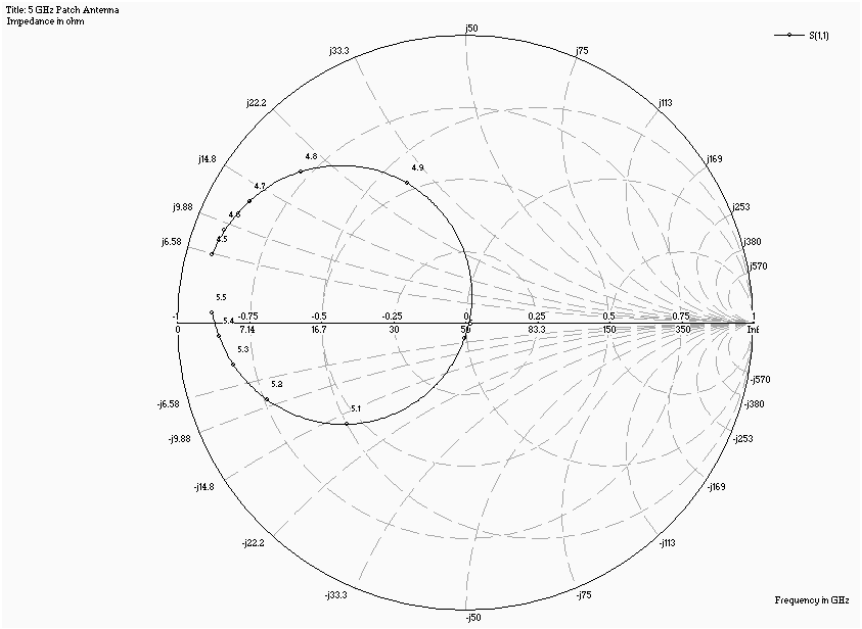

Figure 29. The 5.0 GHz patch antenna Smith chart.

In the final simulations just before an antenna design from the simulations were defined as ready, the brass frame was also introduced in the simulations to see if the antenna characteristic changed. The introduction of the brass frame did not influence the simulation results much.

The dimensions for the antennas from the simulations are:

Antenna [GHz]	Length [mm]	Width [mm]	Distance [mm]	Type
0.9	44.8	6.0	5.2	PIFA
2.4	16.4	4.0	1.6	PIFA
5.0	30.2	8.0	4.7	Patch
9.0	15.8	6.0	1.6	Patch
12.0	11.2	6.0	1.0	Patch

The distance in the table is the distance from the centre of the ground connector to the centre of the signal feed connector in the case of PIFA. In the case of patch antenna it is the distance from the end of the strip to the centre of the signal feed connector

3.2.3.2 The Antenna Manufacture

The source material for the antenna boards is a glass-fibre substrate (1.55 mm) covered with sheets of solid copper on both sides. On the upper side the copper is removed to form an antenna strip. The copper sheet on the upper side is also left as a frame for electrical contact to the brass frame. For the purpose of making an electrically tight shield test device, the edges of the antenna board are covered by copper soldered to the ground plane on the bottom, and to the copper frame on top of the board. An informative illustration is in Figure 30. The manufactured antenna board has got more screw holes than the illustration hint. A standard SMA connector was used for the signal feeding.

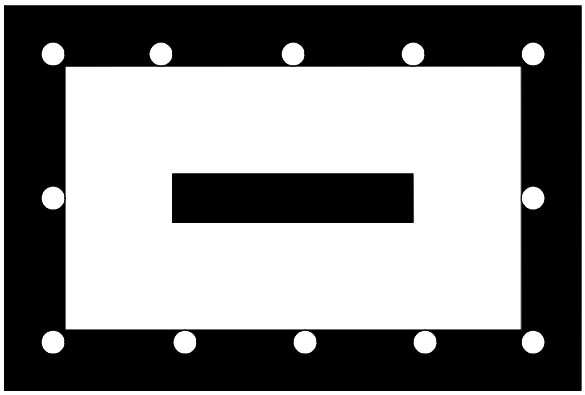

Figure 30. The upper side of the antenna board with the antenna strip in the centre and the surrounding copper frame with holes for screws.

3.2.3.3 The Antenna Verification

Directly after an antenna was manufactured its SWR was measured. Even if the antenna was manufactured exactly as the simulation indicated the result was not always perfect. Minor adjustments had to be done to the manufactured antennas, such as shorting the metal strip length or changing the distance between the connections. The expected major contribution to the difference from simulation to the manufactured antenna was the fact that the electrical properties of the glass-fibre substrate are depending on the frequency; the only available data was for a specific frequency.

The SWR measurements sometimes revealed that it was easier to define a new working frequency for the antenna than trying to manufacture an antenna matched exactly to the specified frequencies. The 0.9 GHz PIFA worked at the specified frequency. The 2.4 GHz PIFA proved to be best at 2.2 GHz. The 5.0 GHz patch antenna was almost perfectly matched to its specified frequency. The 9.0 GHz patch antenna was defined to be a 9.4 GHz antenna (later changed to 8.8 GHz). The 12.0 GHz patch antenna was best matched at 12.3 GHz. The SWR measurements were performed with the brass frame mounted without shield holding board.

4 The Verification of the Measurement System

4.1 Verification

The verification of the shield test measurement system is the process of testing it. The final objective for the test is to find out if the shield test measurement system is reliable.

The following passage describes the initial set-up and the adjustments leading to the final set-up.

4.1.1 The Initial Set-up

The initial measurements were performed in a straightforward approach. The shield test device was put in the anechoic chamber on an existing fixture for antenna radiation pattern measurements. Both the signal generator and spectrum analyzer were located outside the anechoic chamber because of the obvious convenience in controlling the measurements from there. The signal generator fed the shield test device using existing signal cables and arrangements for getting the signal through the walls of the anechoic chamber. The set-up is illustrated in Figure 31.

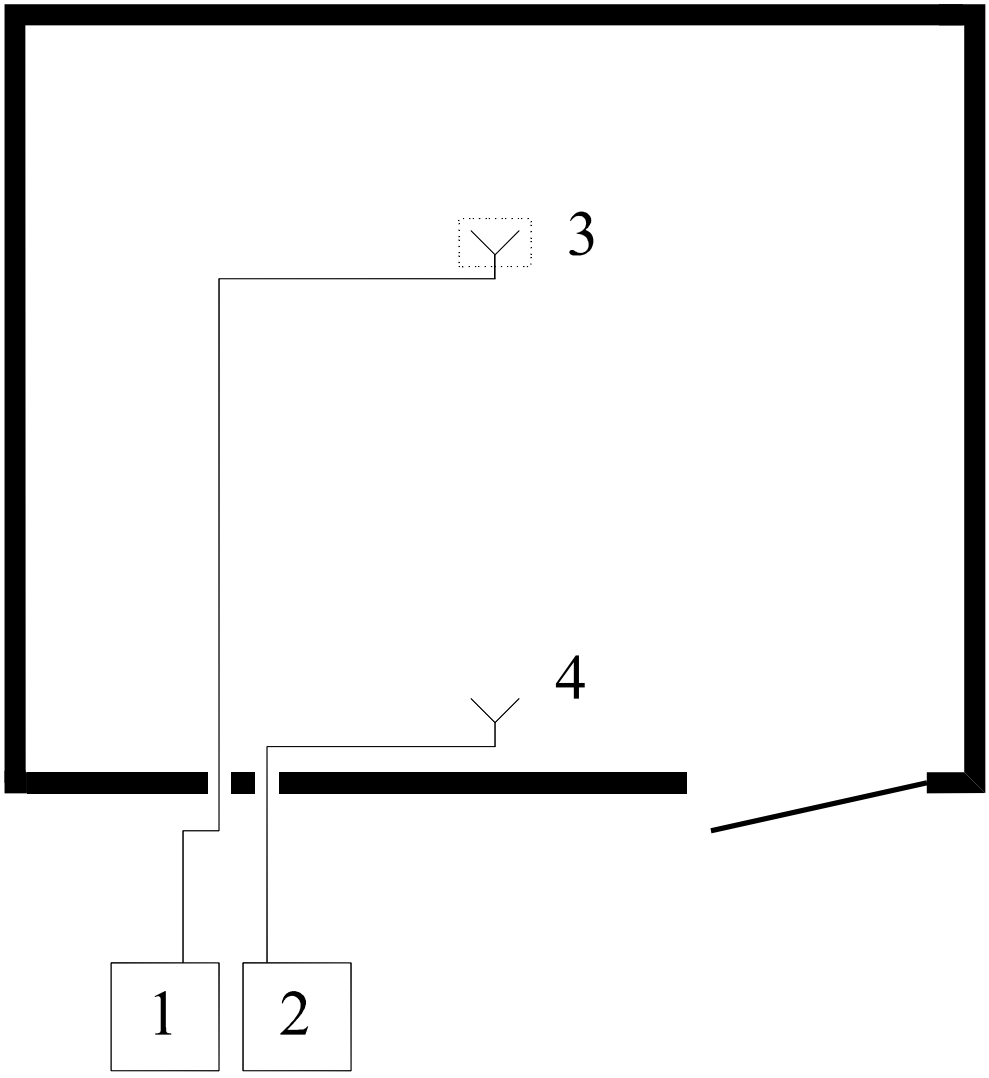

Figure 31. The initial set-up. 1. Signal Generator, 2. Spectrum Analyzer, 3. Shield Test Device, 4. Receiving antenna

Since the 0.9 GHz antenna was the only antenna manufactured at the time, the measurements were limited to that frequency. The purposes of the initial measurements were to find out if the antenna worked and if the measurement system was able to detect a difference between different shielding materials.

The distance from the shield test device to the receiving antenna was 3 meters.

When testing if there was any leakage from the shield test device, the shield holding board was shifted to a board with a solid layer of copper called closed shield test device. The result was compared to a removal of the shield test device from the feeding and a 50-Ohm termination inserted in its place. If the shield test device was leaking, the received signal level when closing the shield test device should differ from the received signal when the termination was in its place.

The 50-Ohm termination test could also tell if there was any leakage in the signal path from the anechoic chamber wall to the shield test device.

The above tests were performed to make sure it was possible to detect the shielding effectiveness of the material intended for test.

Several test configurations were measured:

Open:	The shield test device without shield holding board
Cavity Board:	The shield test device without shielding material
Shield Test:	The shield test device with shielding material in place
Closed:	The shield test device with shield holding board without cavity shape
Terminated Cable End:	50-Ohms termination instead of the shield test device

The open shield test device measurement indicates the maximum signal peak. When the shield holding board is mounted it is possible to detect if the received signal level is decreased compared to the open shield test device measurement.

The measurement with applied shielding material was compared to the measurement with shield holding board mounted. The difference in signal level reveals the SE of the shield material under test during the test conditions.

4.1.2 Progress

This section describes the progress from the initial set-up to the final set-up. The descriptions include a short summary of the problem and the tried out solution.

1. Leaking signal feed cable.

The original signal feed cable was the cable used for ordinary antenna measurements. From the received signal levels the conclusion was clear: the signal path is leaking somewhere inside the anechoic chamber, most possible in the rotary joint in the bottom of the turntable. The turntable was not used for rotation initially so another cable could easily bypass the rotary joint.

2. Change of signal feed cable.

A 4.5 meters cable for use as signal feeding cable was joined from several BLQB signal cables. The joined cable reaches from the anechoic chamber wall directly to the shield test device. The tests for frequencies lower than or equal to 2.2 GHz reveals no leaking feed signal. However, the received signal was too weak (not distant enough from the noise level) when testing candidate shield materials.

3. Use of amplifiers.

One low noise amplifier (LNA) was inserted in the detection signal path almost directly outside the anechoic chamber. The received signal now seemed strong enough but when trying at the high frequencies, 9.4 GHz and 12.3 GHz, the signal was still too weak. Another LNA had to be inserted in series after the first one. Their combined amplification was about 50 dB.

4. Unwanted signal path.

After the amplifiers were inserted a new leakage was discovered. Even if the signal feed were terminated at the terminal immediately inside the anechoic chamber a signal could be seen at the spectrum analyser at the feeding frequency. Possible parasite signal paths were considered but the

solution proved to be change of signal cables outside the anechoic chamber from BLQB ones to Suhner Sucoflex 100 ones and longer physical distance from the signal generator to the amplifiers and the spectrum analyzer.

4. Low signal level discovered.

Even when the amplifiers were used the received signal level was unexpectedly low. No shielding material was attenuating the signal path from the shield test device antenna and the detection RX antenna. Still the signal level was too low at high frequencies 9.4 GHz and 12.3 GHz. The attenuation in the BLQB cable was measured to differ around 25 dB from 2 GHz to 12 GHz. The cables inside the anechoic chamber were changed to Suhner Sucoflex 100 ones. The attenuation now seemed to be reasonable even at the high frequencies.

5. Reflection problems

The antennas up until 5.0 GHz show no leakage but the antennas for higher frequency show leakage. After some discussions regarding the leakage, it was proposed that there might be high SWR from the antenna board in some cases. Unfavourable SWR can cause leakage from the antenna board. From earlier experience by the experts they introduce a 3-dB attenuation just before the feeding of the shield test device. The attenuator reduces the leakage but it is not eliminated.

6. Extra investigation of the SWR.

Because of the possible antenna reflection problems extra SWR measurements of all the antennas and all measurement cases were performed. It revealed that the antenna used at 9.3 GHz is less problematic at 8.8 GHz. The tested cases were: open shield test device, closed shield test device, shield holding board, mounted plastic cap and mounted steel cap. The change of antenna frequency further decreased the leakage problems.

7. Unstable measurement results.

The results seen from early measurements can not be reproduced even if only the relative signal levels are compared. It was expected that the physical orientation of the shield test device was the factor making the received signal level fluctuate the way they did. A possible bypass of this problem was to start the turntable and make 3D radiation patterns. It soon proved very time consuming to control the turntable manually and meanwhile write down the received signal levels from the spectrum analyzer.

Sometimes there was some leakage in the signal path as well and this led to the possibility of moving the signal generator from outside of the anechoic chamber to the inside of the anechoic chamber at the turntable.

8. Putting the signal generator inside the anechoic chamber.

By placing the signal generator at the turntable, the length of the signal path from the signal generator to the shield test device was minimised.

Extra controls of the tightening of all joints proved to improve the stability in the measurements. The joints had not been tightened so forceful earlier.

9. Computer controlling the set-up

The purpose of the computer controlling of the measurement set-up was to be able to get radiation patterns to confirm the direction sensibility of the shield test device.

Due to the time consumption of collecting radiation pattern data manually and the uncertainties of possible reading faults, existing control software is modified to shield testing. The computer outside the anechoic chamber was equipped with GPIB (General Purpose Interface Bus) and LabView software. The computer software was via GPIB controlling the turntable, the turn device and the spectrum analyzer. The placement of the signal generator inside the anechoic chamber made it almost impossible to frequency synchronise the spectrum analyzer to the signal generator. They had not been synchronised in earlier measurements. When the set-up was computer controlled the spectrum analyzer must use a wider span and then read the maximum value in that span to tolerate drifting frequencies.

The computer controlled data gathering made it easier to measure and present antenna diagrams and to find the maximum signal level in any direction. The simplicity and fastness of a computer controlled system permits an extension of the measurements to three dimensions; it was not practically possible to do that manually.

4.1.3 The Final Set-up

The final set was developed from the initial set-up. All measurements were performed inside an anechoic chamber. The shield test device was mounted to a fixture placed at a turntable. The shield test device could be rotated 360 degrees in the vertical plane and the turntable could rotate 360 degrees in the horizontal plane. This allowed the radiation pattern from the shield test device to be measured in three-dimensions (3D). A computer outside the anechoic chamber controls the rotations. The signal generator was located inside the anechoic chamber at the turntable. The final set-up is illustrated in Figure 32.

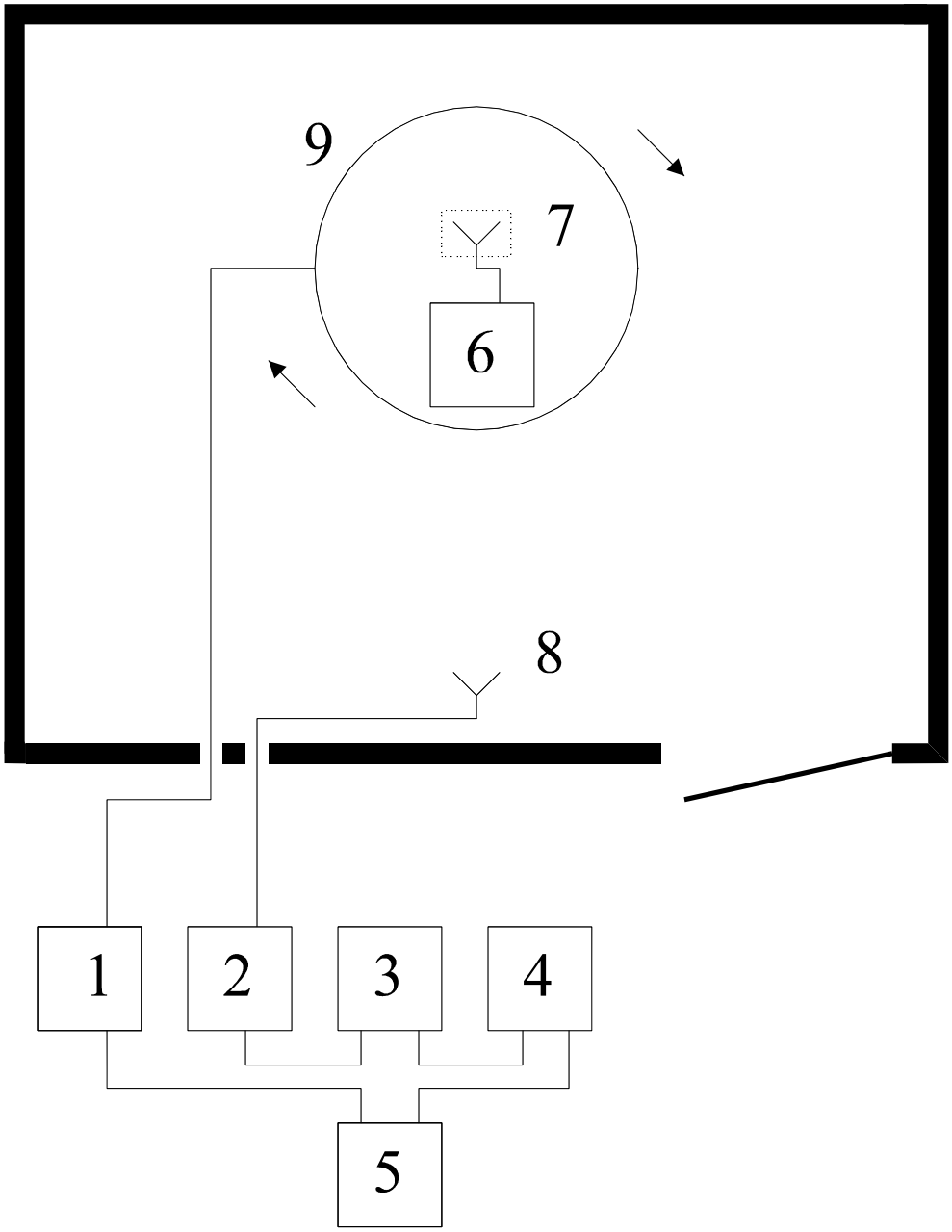

Figure 32. The Final Set-up. 1. Control Device for Turntable, 2. Low Noise Amplifier, 3. Low Noise Amplifier, 4. Spectrum Analyzer, 5. Computer Controlling Measurements, 6. Signal Generator, 7. Shield Test Device, 8. Receiving Antenna, 9. Turntable

Special arrangements were made for the power supply to the signal generator. There was no connecting plug at the turntable or anywhere close it so a special suspension device had to be constructed, see Figure 33. The power line probably influenced the measurements in some way but not in a disruptive way.

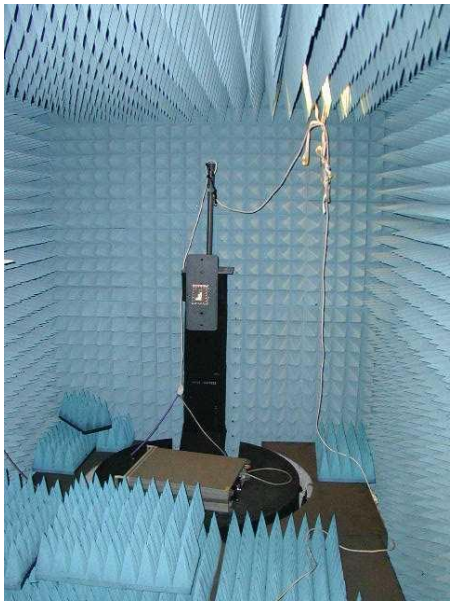

Figure 33. Fixture for shield test device.

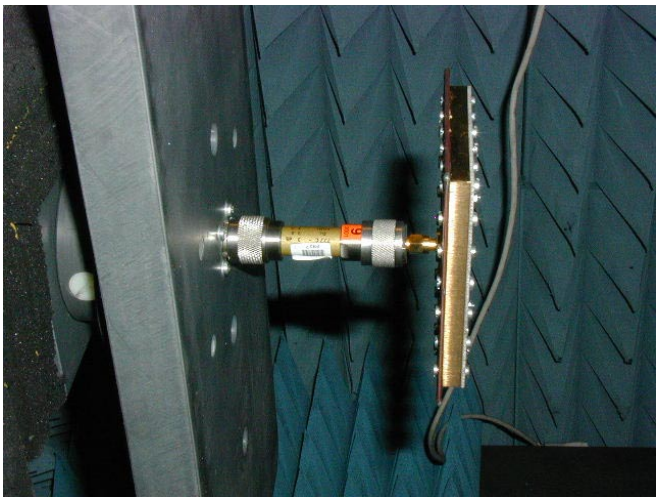

Figure 34. The connection from the rotary joint to the shield test device. The 3-dB attenuator is seen between the rotary joint and the shield test device.

The signal generator was connected to a Suhner Sucoflex 100 cable leading up to the rotary joint in the fixture. On the other side of the rotary joint there was a 3-dB attenuator just before the connection to the shield test device. The attenuator reduced the reflections from the shield test device antenna in case of impedance mismatch. The attenuator can be seen in Figure 34.

The signal generators fed the antenna inside the shield test device with 10-dBm. Two signal generators had to be used due to their individual frequency limitations

The receiving antenna was a conical log-spiral antenna placed 3 meters away from the shield test device on the same vertical level. The receiving antenna was connected to a 3-dB attenuator and further to a cable leading to a connector through the wall of the chamber. The stand holding the receiving antenna is seen in Figure 35.

Figure 35. The conical log-spiral receiving antenna.

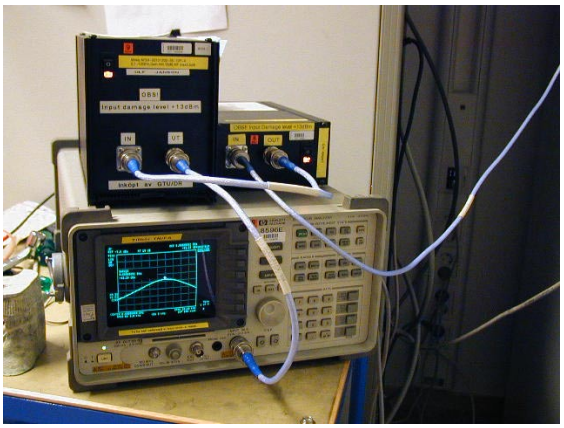

Figure 36. The detection equipment outside the anechoic chamber.

The signal detection equipment was placed outside of the anechoic chamber. The received antenna signal was quite weak and it was therefore amplified before a spectrum analyzer was able to detect the signal in all cases. Two series connected low noise amplifiers (LNAs) performed the amplification, see Figure 36.

The data collection was computer controlled; the computer was equipped with a General Purpose Interface Bus (GPIB) and controlled the rotations of the shield test device and the reading of the spectrum analyzer.

The computer software for data gathering can present the result in diagrams, see Figure 37.

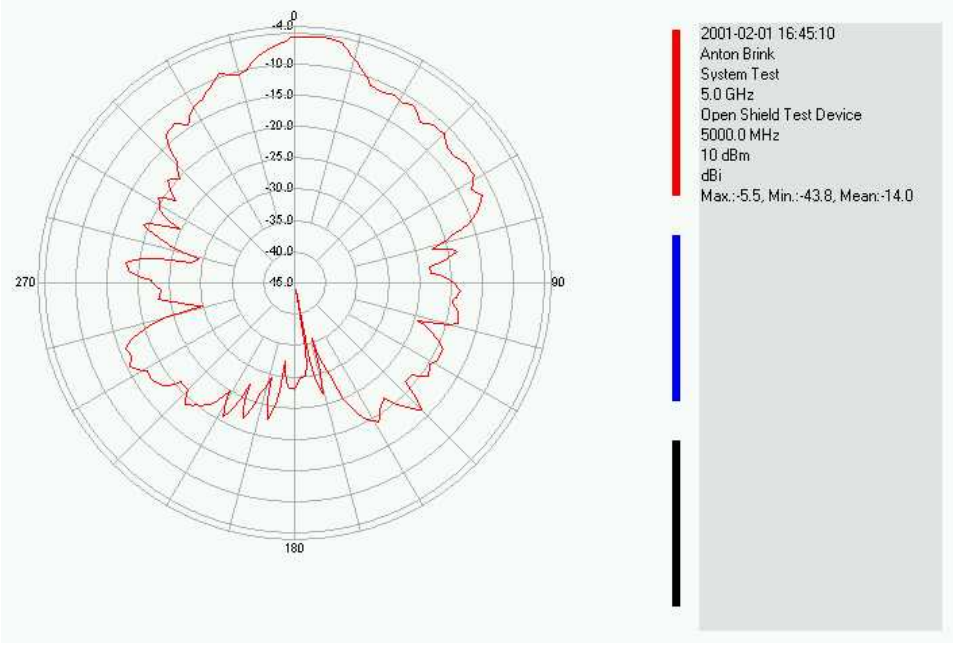

Figure 37. Example of antenna radiation pattern from open shield test device.

The gathered data can also be processed in Matlab and displayed as a rotating 3D figure. One useful processing is the possibility to find the maximum radiation from the 3D sphere.

4.1.3.1 The Degradation Test

Tests were carried out to see if it is possible to degrade a shielding material in some controlled manner to study if the test system is sensible enough to detect any differences. The tests were conducted in the following way:

- A shield material was attached to a shield holding board.
- The shield material was tested at all test frequencies in the shield test system.
- The shield material was degraded in a controlled way; an eleven-mm slit was cut in the shield material.
- The degraded shield material was tested at all test frequencies in the shield test system.
- The results from the original material test were compared with the degraded material test.

The easiest comparison was to study the radiation pattern presented from the software controlling the 3D measurements. Degraded materials do probably radiate more than the original material in some direction.

The second easiest comparison was to study the maximum value from the log file created when the 3D measurements were performed. The maximum value was found by use of Matlab.

The plastic shield degradation measurement results are presented in Appendix E. The result is ambiguous; the SE gets better for low frequencies after degradation. The diagram results can be compared to the maximum values dragged out from the 3D data by use of Matlab, shown in the following table.

	Degradation differences:				
	0.9 GHz	2.2 GHz	5.0 GHz	8.8 GHz	12.3 GHz
Original [dBm]	-27	-30	-38	-35	-39
Degraded [dBm]	-30	-23	-28	-29	-31
Difference [dB]	3	-7	-10	-6	-7
11 mm in wavelength for the frequencies.	0.03	0.08	0.18	0.32	0.45

When studying the absolute signal level in the above table or in the diagrams in appendix, it is good to know that the free-room attenuation is frequency dependent.

$l = 20 \cdot \log_{10}(4 \cdot \pi \cdot d/\lambda)$;l=attenuation in dB, d=distance in meters, λ=wavelength.

The free-room attenuation for signals at a 3 meters distance are calculated below:

Frequency [Hz]	0.9 GHz	2.2 GHz	5.0 GHz	8.8 GHz	12.3 GHz
Attenuation [dB]	41	49	56	61	64

4.1.4 Sources of Error

Application of the shielding material:
Some shielding materials are very sensitive to their application to the shield holding board. The electrical contact between the shield material and the shield holding board must be ensured.

Leaks in the cable joints in the anechoic chamber:
The joints between the cables leak but the effect can sometimes be reduced by use of signal absorbing material above the joints.

Repeatability between measurement series:
The received signal level is dependent of the physical orientation of the shield test device. The stability of the measurements would be improved by use of water level then mounting the shield test device. The use of 3D measurements reduced the effect of less precise initial mounting.

The rotary joint:
The rotary joint in the bottom of the turntable is not isolating the signal good enough for the shielding measurements. The rotary joint must be bypassed.

SWR-differences:
The antenna SWR changes according to environment changes in the shield test device due to different shielding materials. The SWR can change considerable from one material to another

material. This makes the radiated signal level from the antenna inside the shield test device dependent on the material in test, which is an unwanted property of the system.

Unwanted signal paths:
In the beginning signal flowed directly from the signal generator to the spectrum analyser through the air. Then the signal generator was moved further apart from the signal cables connecting the receiving antenna to the amplifiers the effect disappeared.

4.1.5 Analysis

If one tested shield material has lower radiation mean than another tested shield material it is easy to determine which one to use if not:
The material with the lowest mean has its maximum radiation in a direction greater than the maximum radiation of the other material with a higher overall mean.

The suggested situation might be rare but it might occur and by then there are ambiguous results to use for the material evaluation. There can be situations where it must be considered which is best: lowest mean or lowest maximum radiation.

To determine the reliability of the test system a lot of measurements were carried out. The shield materials were tested at all frequencies showing ambiguous results. Even if the same shield holding board had the very same shield cap mounted and shifted to all shield test devices the results changed over time (time is in this case a week). This phenomenon made it highly uncertain if the shield test system was reliable. Other measurements such as measurements of the shield holding board without mounted shield cap tends to be stable over time and also the isolation test proved to be stable.

This behaviour of the measurement results gave attention to how the shield holding board was treated between the measurements. The shield holding board had not been cautiously handled between the measurements and it was expected that the shielding performance were affected by the rough treatment. It is also crucial to find the correct way of mounting a shield cap to the shield holding board before doing a serious material investigation.

The LabView program can present the measurement data in a diagram showing the radiation from the shield test device in a two-dimensional plane. The data can also be imported into Matlab for further processing; rotating 3D plots can be shown using existing Matlab extensions, see Figure 38.

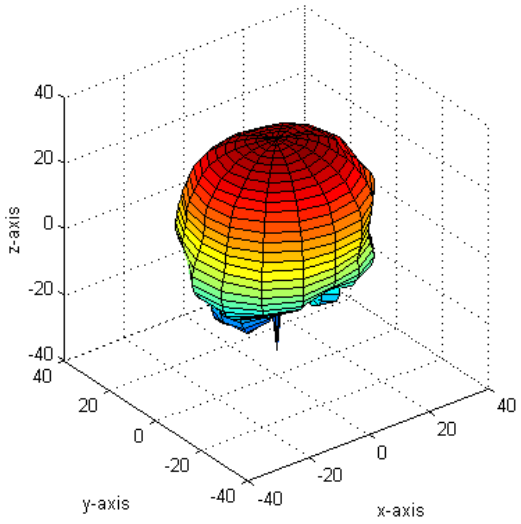

Figure 38. Matlab 3D radiation pattern.

4.1.6 Shield Material Measurements

The measurement system can be used in shield material tests. The tests are supposed to be performed in the following way:

- The shield holding board is prepared with a candidate shield material.
- The shield material is tested at all available frequencies.
- The radiation data is compared to measurements of the shield test device with no shield holding board mounted.
- The radiation data can also be compared to other materials radiation data and the materials can be referred to each other, relative measurement.

4.1.7 Tips

The radiation pattern for low frequencies, around 900 MHz, seems to be affected by the physical orientation of the things inside the anechoic chamber. In one measurement an extra signal generator was put on top of the first one and at the 900 MHz measurement the shape of the signal generator could actually be "seen" in the antenna pattern. Absorption material piled up on the floor is probably influencing the results in the same way. So it is probably important to find a set-up before the measurements start and try not to disturb it too much physically.

It might be better to change the antenna board instead of the shield holding board when the tests are carried out. By doing so the shield material will be much less affected by mechanical stress during the test cycle. The test might be more reliable in this way.

The use of conductive grease as gasket material did not improve the shield test device tightness. The closed shield test device is at all tested frequencies not leaking considerably more than if the shield test device is replaced by a 50-Ohm termination. As an example, the system tightness at 5.0 GHz is seen in Figure 39. No conductive grease was used between the brass frame and the board closing the shield test device during the example measurement.

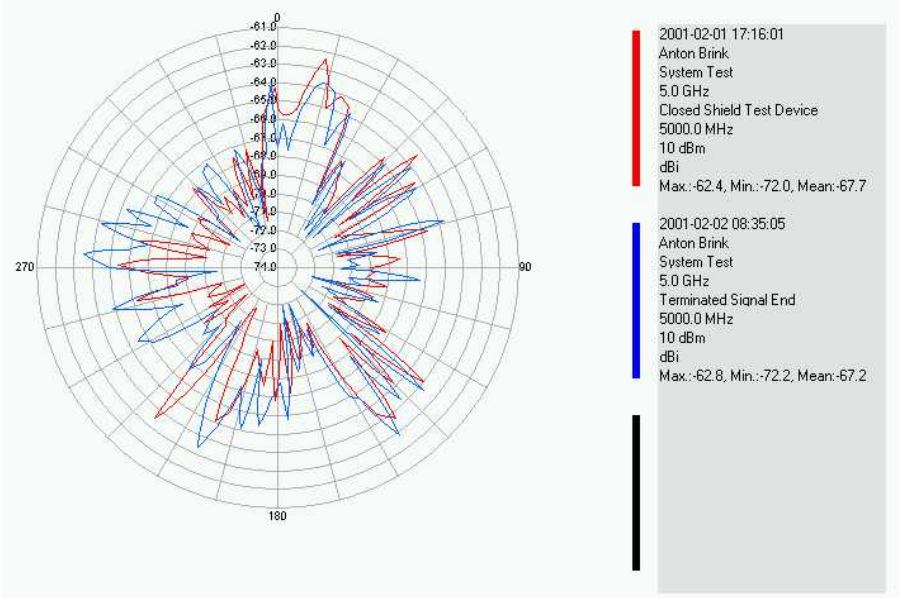

Figure 39. The closed shield test device is not leaking considerably more than if the shield test device is replaced by a 50-Ohm termination

Figure 40 is presented as an illustration of the distance in signal levels from a shield test measurement to a measurement of the closed shield test device.

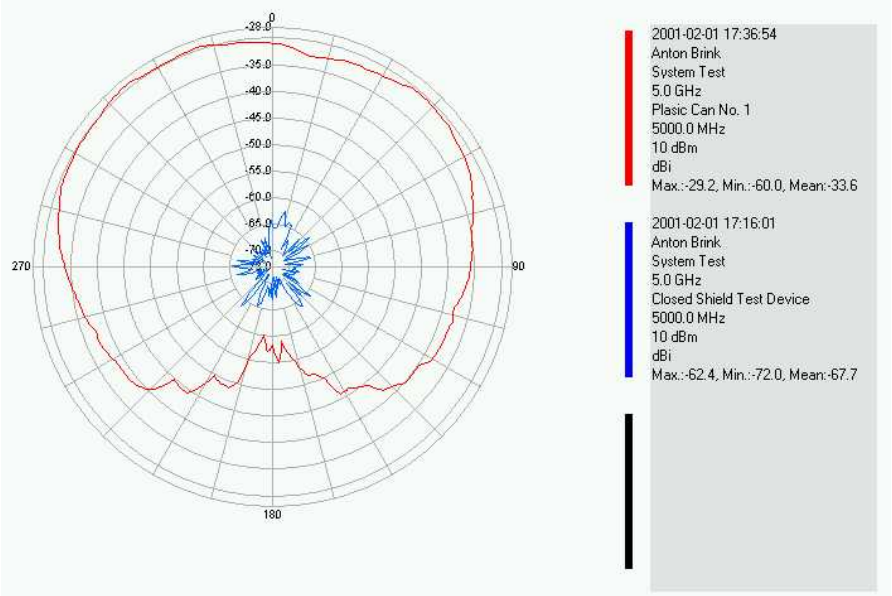

Figure 40. The received signal level from a shield material measurement was considerable stronger than the received signal level from a closed shield test device.

5 Conclusions

5.1 Summary

In the beginning of the work for this master's thesis it was uncertain if the thesis would end in something useful. The task was to gather shielding theory in a written theory section and to design a shield test measurement system in the rest of the time.

The theory part explains shielding conceptions, such as:

Shielding Effectiveness
Electromagnetic Interference
The difference between near fields, far fields and plane waves
Radiation from apertures
Reflections from practical shielding work

There are some useful formulas in the theory part for estimations of leakage from apertures.

The design of the shield test measurement system was time consuming but at last a success. The designed system parts can be used for measurements investigating the performance of new shielding materials. The measurements can reveal differences in shielding effectiveness for different materials, and do so in a broad frequency band.

The design process was anything but straightforward, a lot of problems were discovered in the work to find a stable and reliable measurement set-up for the system.

A reflection from the initial work for finding a stable system is quoted below:

"Initially the measurement system had no amplifiers mounted before the spectrum analyser. At low frequency, 900 MHz, the received signal was sufficiently high even without amplification. The results looked very promising in the beginning, but later when it was thought it would be easy to make all measurements repeatable the problems accelerated. Some times the results were almost unambiguous but sometimes they were highly ambiguous. A lot of tests had to be performed until there were even the slightest possibility for repeatability. Even the results changed over time, which did not seem promising."

But after the adjustments leading to the final set-up the author declares that:

"It is absolutely clear that the test system can detect and document differences from one shielding material to another one. It is also possible to degrade a material in a controlled way and see differences in the received signal levels. "

The final measurements are repeatable and stable over time (limited testing time).

The system allows Ericsson to perform shielding effectiveness measurements of new candidate materials for mobile phone shielding. Test result data show the relative performance between different materials. The measurements give a foundation for better decisions regarding choice of shielding material. The result of better decisions is faster and cheaper product development. The engineers do not have to be stuck in quasi discussions regarding which shielding material to use

in a project. The discussions used to be based on weak assumptions of material properties. Now there is a measurement evaluation to refer to in case of a dead lock in the discussion.

5.2 Future Improvements

In the future more accurate positioning of the shield test device should be considered. A more precise positioning will probably give less fluctuating received signal levels.

When carrying out a shield material evaluation for a mobile phone project there must be an ongoing discussion with the shield material producer. The discussion aims to find out if the shield material is correctly joined to the copper on the shield holding board. During the measurements presented in this thesis no contacts with the shield material manufacturers have secured the correctness of the joining of shield materials to the shield holding board. It is assumed that the plastic material is more sensitive than the steel material for the application to the shield holding board. There are a lot of factors that can be varied then fastening the plastic material. All factors must be discussed with the manufacturer when a shield material evaluation will be carried out.

The presentation of the results may be improved in the shield measurement program. It is valuable to make a function to present a selectable cross-section of the radiation pattern and not as now only the initial cross-section. The best thing to implement is an automatic function to select the cross-section with the maximum received amplitude. The addition of LabView code can not be very large.

6 Acknowledgements

I would like to thank the antenna design department at Ericsson for their help and support before and during my shield test measurements.

I send thanks to the GUB/DR department and especially my tutor Per-Anders Svensson and Staffan Iveberg.

Specials thanks to my supporting tutor at Lund Institute of Technology, Daniel Sjöberg.

The prototype workshop at Ericsson helped me a lot in the manufacturing of the shield test device.

7 References

7.1 Bibliography

[1] Aas, Jon Anders, *Antenneteknikk*, NTNU, 1997

[2] Cheng, David K., *Field and Wave Electromagnetics*, Addison-Wesley Publishing Company Inc., 1989

[3] Chomerics, *EMI Shielding for Commercial Electronics*, Chomerics, Dec. 1997, USA

[4] Clupper, T., Wheeler, J., *"Correlating DC resistance to the shielding effectiveness of an EMI gasket"*, W.L. Gore & Assoc., Inc., 1999, USA

[5] Daher, J. K., Denny, H. W., *"Evaluation of shielding effectiveness test methods for conductive plastics"*, Plastics in Telecommunications III. Plastics & Rubber Inst, UK, 1982, pp. 30/1-10

[6] Field, J C G, *"An introduction to electromagnetic screening theory"*, Inst. Elect. Eng. Colloq. Screening Shielding, U.K., Nov. 1983, pp. 1/1-1/15

[7] Hemming, Leland H., *Architectural electromagnetic shielding handbook*, IEEE Press, New York, 1992

[8] Hudak, Shane, *"EMI shielding strategies- proper design and attachment options"*, RF Design, pp. 54-62, December 1997

[9] Jerse, Thomas A., *"Shielding Basics"*, RF Design, pp. 83-88, March 1990

[10] Kunkel, George M., *"Electromagnetic Leakage Through Slot Configurations in a Shielded Enclosure"*, Chicago 1994. Compatibility in the Loop. IEEE International Symposium on EMC. Symposium Record, IEEE, New York, NY, USA, 1994, pp. 274-8

[11] Medveczky G.G., Dickten T., *"High quality shielding with predictable and verifiable effectiveness"*, 1999 IEEE International Symposium on Electromagnetic Compatibility. Symposium Record, IEEE, Piscataway, NJ, USA, 1999, 2 vol. 1050 p. pp. 565-70

[12] Ott, Henry W., *Noise reduction techniques in electronic systems, second edition*, Wiley-Interscience, 1988

[13] Paul, Clayton R., *"Radiated and Conducted Emissions"*, In Perez, Reinaldo, editor, *Handbook of Electromagnetic Compatibility*, Academic Press, 1995

[14] Pozar, David M., *Microwave engineering, second edition*, Wiley, 1998

[15] Schulz, Richard B., *"Electromagnetic Theory and Fundamentals of EMC"*, In Perez, Reinaldo, editor, *Handbook of Electromagnetic Compatibility*, Academic Press, 1995

[16] Tsaliovich, Anatoly, *Electromagnetic shielding handbook for wired and wireless EMC applications*, Kluwer Academic Publishers, 1999

[17] Wilson, P. F., Ma, M. T., *"Factors influencing shielding effectiveness measurements"*, International Symposium on Electromagnetic Compatibility, IEEE, New York, NY, USA, 1985, 629 p. pp. 29-33

7.2 Appendix A

7.2.1 Acronyms and Abbreviations

3D	Three Dimensions
BLQB	Brown Low Quality Bulk
CAD	Computer Aided Design
dB	decibel
dBm	decibel, 1 mW reference
DC	Direct Current
EM	Electromagnetic
EMC	Electromagnetic Compatibility
EMI	Electromagnetic Interference
GPIB	General Purpose Interface Bus
GSM	Global System for Mobile communications
ITU	International Telecommunication Union
LNA	Low Noise Amplifier
mW	milli Watt
Nm	Newton meter
PCB	Printed Circuit Board
PIFA	Planar Inverted F Antenna
RF	Radio Frequency
RX	Receive
SE	Shielding Effectiveness
SWR	Standing Wave Ratio
TE	Transverse Electric waves
TEM	Transverse Electromagnetic waves
TM	Transverse Magnetic waves
TX	Transmit

7.3 Appendix B

7.3.1 Skin Effect

The skin effect is a frequency-dependent material property. It tells the attenuation of the material and is dependent of the conductivity, σ, and permeability, μ. The skin depth δ is defined as the distance that the wave has to travel for it to be attenuated 1/e or 37 percent of its original amplitude.

$$\delta = \sqrt{\frac{2}{\omega\mu\sigma}} = [m]$$

From the formula it can be seen as the frequency increases the skin depth gets shallower. This indicates better attenuation for the shield.

7.3.2 Standing Wave Ratio

Standing waves is a well-known physic phenomenon. When a wave is reflected the resulting wave consists of a superposition of the incident and the reflected wave; such waves are called standing waves. The coefficient of reflection is called Γ. A definition of the mismatch is the voltage standing wave ratio (VSWR); which is bounded by the reflection coefficient $-1 \le \Gamma \le 1$.

$$VSWR = \frac{V_{\max}}{V_{\min}} = \frac{1+|\Gamma|}{1-|\Gamma|}$$

$$1 \le VSWR \le \infty$$

VSWR=1, or Γ=0, implies a matched load, i.e. no reflection. [14]

7.3.3 Wave Impedance

The wave impedance (Z_W) is defined as the ratio of the electric field amplitude (E) to the magnetic field amplitude (H).

$$Z_W = \frac{E}{H}[\Omega]$$

The characteristic impedance (Z_C) of a medium is a function of the constitutive parameters of the medium and the frequency of the electromagnetic wave. The characteristic impedance can be expressed as:

$$Z_C = \sqrt{\frac{j\omega\mu}{\sigma + j\omega\varepsilon}}[\Omega]$$

For air ($\sigma=0, \mu=\mu_0, \varepsilon=\varepsilon_0$), the characteristic impedance is $Z_0=377\Omega$. To be effective, the shield's characteristic impedance, Z_S, must either be very much larger than 377 ohms or must be very much smaller. The latter condition is easier to realise, i.e., $\sigma >> \omega\varepsilon$; for this case, Z_S becomes:

$$Z_S = \sqrt{\frac{j\omega\mu}{\sigma + j\omega\varepsilon}} \approx \sqrt{\frac{j\omega\mu}{\sigma}} = (1+j)\sqrt{\frac{\omega\mu}{2\sigma}}[\Omega]$$

The magnitude of the shield impedance

$$|Z_S| = \sqrt{\frac{\omega\mu}{\sigma}}[\Omega]$$

should be quite small over a wide range of frequencies, since σ is assumed to be large.

For insulators (σ<<ωε) the characteristic impedance is independent of frequency and becomes

$$Z = \sqrt{\frac{\mu}{\varepsilon}}[\Omega]$$

The wave impedance near a simple magnetic-field source is given by:

$$Z_{W,H} = -j\omega\mu_0 r[\Omega]$$

The wave impedance near a simple electric-field source is:

$$Z_{W,E} = \frac{1}{j\omega\varepsilon_0 r}[\Omega]$$

As a wave propagates away from either source, Z_W asymptotically approaches 377 ohms in the far field. [9]

7.3.4 Wavelength

The wavelength for any frequency:

$$\lambda = \frac{c}{f}[m]$$

λ=Wavelength [*m*]
c=speed of light [*m/s*]
f=frequency [s^{-1}]

7.4 Appendix C

7.4.1 Wave Impedance Formula Derivation

$$E_p = \lim_{n\to\infty}\left[\frac{2Z_r}{(1+Z_r)}\cdot e^{-\gamma d}\cdot\frac{2}{(1+Z_r)}\cdot E_1 + \right.$$

$$+\left(\frac{(1-Z_r)}{(1+Z_r)}\cdot e^{-\gamma d}\cdot\frac{(1-Z_r)}{(1+Z_r)}\cdot e^{-\gamma d}\right)\cdot\frac{2Z_r}{(1+Z_r)}\cdot e^{-\gamma d}\cdot\frac{2}{(1+Z_r)}\cdot E_1 +$$

$$+\left(\frac{(1-Z_r)}{(1+Z_r)}\cdot e^{-\gamma d}\cdot\frac{(1-Z_r)}{(1+Z_r)}\cdot e^{-\gamma d}\right)^2\cdot\frac{2Z_r}{(1+Z_r)}\cdot e^{-\gamma d}\cdot\frac{2}{(1+Z_r)}\cdot E_1 +$$

$$\vdots$$

$$+\left(\frac{(1-Z_r)}{(1+Z_r)}\cdot e^{-\gamma d}\cdot\frac{(1-Z_r)}{(1+Z_r)}\cdot e^{-\gamma d}\right)^{n-1}\cdot\frac{2Z_r}{(1+Z_r)}\cdot e^{-\gamma d}\cdot\frac{2}{(1+Z_r)}\cdot E_1 +$$

$$\left.+\left(\frac{(1-Z_r)}{(1+Z_r)}\cdot e^{-\gamma d}\cdot\frac{(1-Z_r)}{(1+Z_r)}\cdot e^{-\gamma d}\right)^{n}\cdot\frac{2Z_r}{(1+Z_r)}\cdot e^{-\gamma d}\cdot\frac{2}{(1+Z_r)}\cdot E_1\right] =$$

$$= \lim_{n\to\infty}\left[E_1\cdot e^{-\gamma d}\cdot\frac{4Z_r}{(1+Z_r)^2}\cdot\left\{1+\left(\frac{(1-Z_r)^2}{(1+Z_r)^2}\cdot e^{-2\gamma d}\right)+\left(\frac{(1-Z_r)^2}{(1+Z_r)^2}\cdot e^{-2\gamma d}\right)^2+\cdots+\left(\frac{(1-Z_r)^2}{(1+Z_r)^2}\cdot e^{-2\gamma d}\right)^{n-1}+\right.\right.$$

$$\left.\left.+\left(\frac{(1-Z_r)^2}{(1+Z_r)^2}\cdot e^{-2\gamma d}\right)^{n}\right\}\right] = E_1\cdot e^{-\gamma d}\cdot\frac{4Z_r}{(1+Z_r)^2}\cdot\sum_{n=0}^{\infty}\left(\frac{(1-Z_r)^2}{(1+Z_r)^2}\cdot e^{-2\gamma d}\right)^n =$$

$$= E_1\cdot e^{-\gamma d}\cdot\frac{4Z_r}{(1+Z_r)^2}\cdot\left[\frac{1}{1-\frac{(1-Z_r)^2}{(1+Z_r)^2}\cdot e^{-2\gamma d}}\right] = E_1\cdot e^{-\gamma d}\cdot\frac{4Z_r}{(1+Z_r)^2}\cdot\left[1-\frac{(1-Z_r)^2}{(1+Z_r)^2}\cdot e^{-2\gamma d}\right]^{-1}$$

By use of logarithm the first term can be modified in the following way:

$$20\cdot\log_{10}\left|e^{\gamma d}\right| = 20\cdot\log_{10}\left|e^{(1+j)\sqrt{\pi\mu\sigma f}\,d}\right| = \left[\delta=\sqrt{\frac{2}{\omega\mu\sigma}}\right] = 20\cdot\log_{10}\left|e^{(1+j)d/\delta}\right| = [see\,below] = 20\cdot\log_{10}e^{d/\delta} =$$

$$= \frac{d}{\delta}\cdot 20\cdot\log_{10}e^{1} \approx 8.686\cdot\frac{d}{\delta}$$

By use of the following expressions:

$$\gamma = \sqrt{j\omega\mu\sigma} = \left[\begin{matrix}\omega = 2\pi f\\ j = e^{j\pi/2}\end{matrix}\right] = \sqrt{2\cdot e^{j\pi/4}}\cdot\sqrt{\pi\mu\sigma f} = \sqrt{2}\cdot e^{j\pi/4}\cdot\sqrt{\pi\mu\sigma f} = (1+j)\cdot\sqrt{\pi\mu\sigma f}$$

$$\left|e^{(1+j)d/\delta}\right| = \left[e^{(1+j)d/\delta}\cdot e^{(1-j)d/\delta}\right]^{1/2} = \left[e^{(1+j)d/\delta+(1-j)d/\delta}\right]^{1/2} = \left[e^{2d/\delta}\right]^{1/2} = e^{d/\delta}$$

7.5 Appendix D

7.5.1 Planar Inverted F Antenna

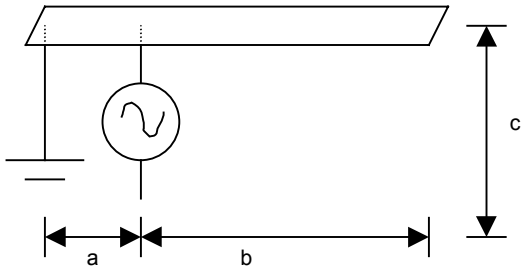

The length $l=a+b$ of the planar inverted F antenna (PIFA) corresponds to ¼λ of the antenna centre frequency. The distance *c* from the antenna strip down to the ground plane will determine the antenna bandwidth. The width of the antenna strip is also influencing the bandwidth but not as much as the height.

The matching of the antenna is very dependent on the distance *a*. The distance *a* corresponds to the distance from the antenna ground connection end to the signal feeding point.

7.5.2 Patch Antenna

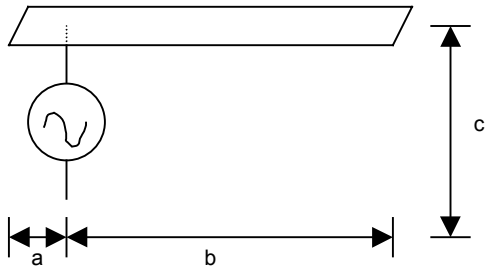

The patch antenna is a simple construction consisting of an antenna strip and a feeding point. The length $l=a+b$ is in this work selected to be ½λ to the corresponding centre frequency. The length *a* is crucial to the matching of the antenna. At the distance *c* beneath the strip there must be a ground plane.

7.6 Appendix E

7.6.1 Plastic Shield Degradation

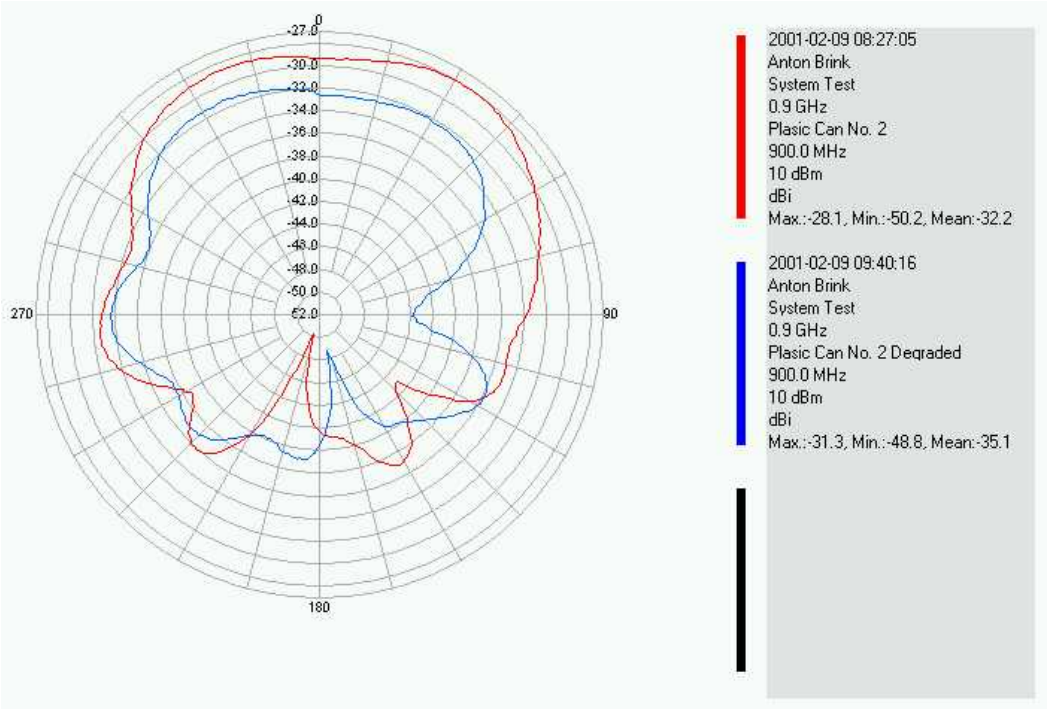

900 MHz measurement of plastic shield degradation.

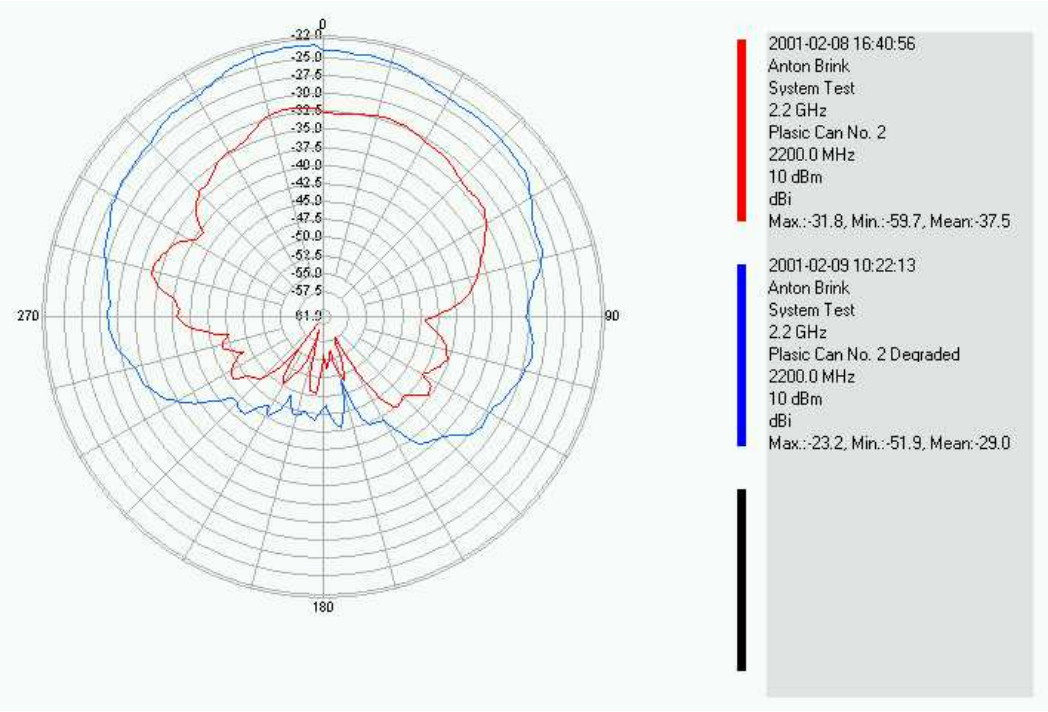

2200 MHz measurement of plastic shield degradation.

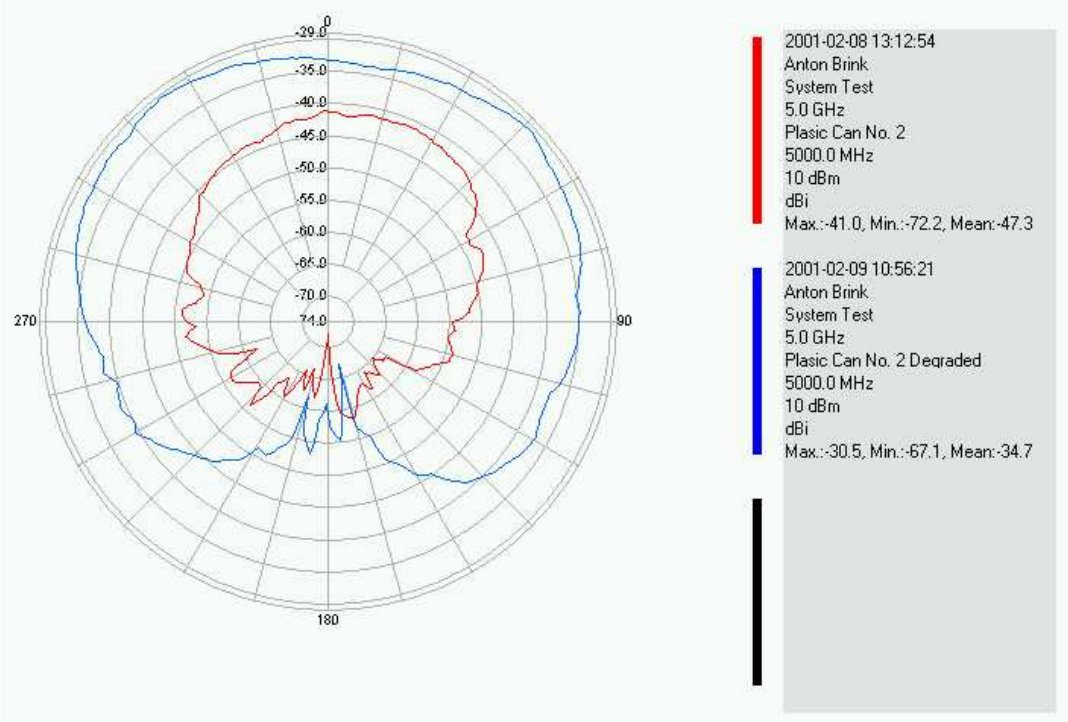

5000 MHz measurement of plastic shield degradation.

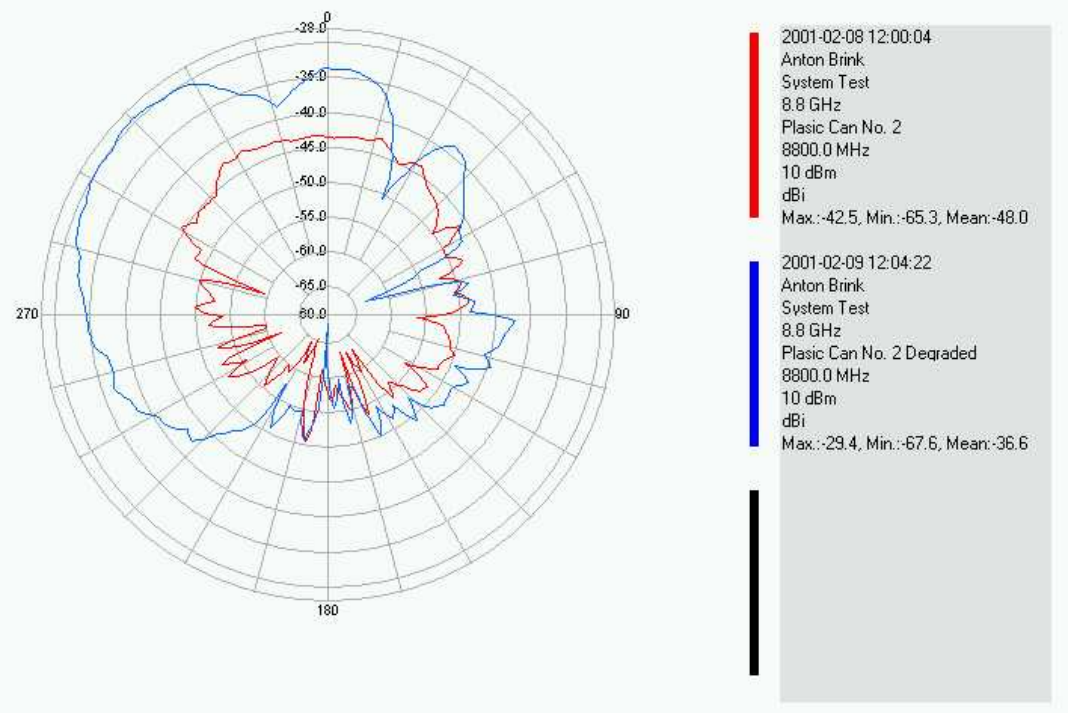

8800 MHz measurement of plastic shield degradation.

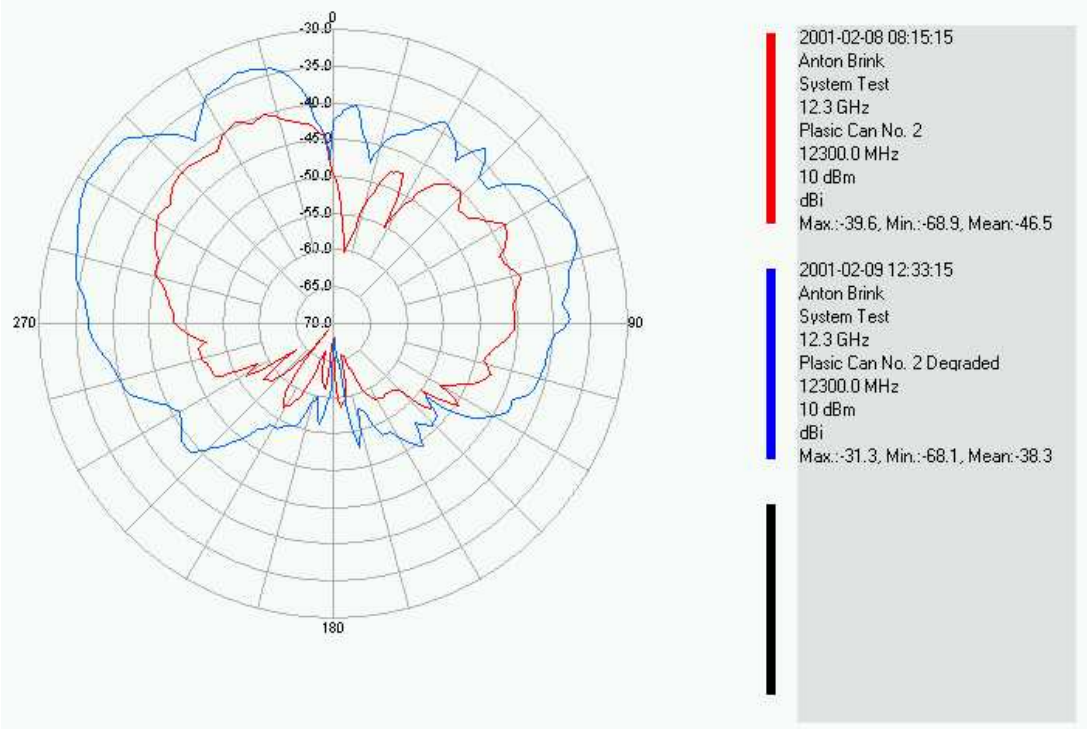

12300 MHz measurement of plastic shield degradation.

7.7 Appendix F

7.7.1 Inventory List

EMCO 3102L Antenna
HP 8596 Spectrum Analyzer
HP 8657B Signal Generator
HP 8671B Signal Generator
MITEC AFS-3 Low Noise Amplifier
MITEC AFS-4 Low Noise Amplifier
Suhner Sucoflex 100 Signal Cable